

**MODELING THE TRANSITION
BETWEEN LYTIC AND LYSOGENIC BEHAVIOR
IN A BACTERIA-PHAGE SYSTEM**

A Thesis
Presented to the
Faculty of
San Diego State University

In Partial Fulfillment
of the Requirements for the Degree
Master of Science in Applied Mathematics
with a Concentration in
Dynamical Systems

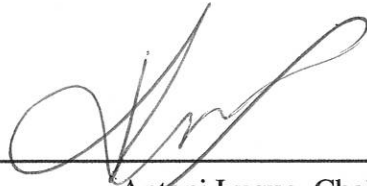
by
Emily Ann Jasien
Summer 2017

SAN DIEGO STATE UNIVERSITY

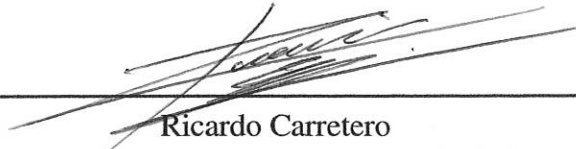
The Undersigned Faculty Committee Approves the

Thesis of Emily Ann Jasien:

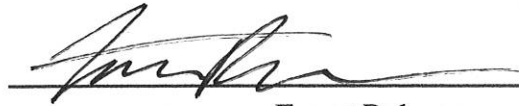
Modeling the Transition
Between Lytic and Lysogenic Behavior
in a Bacteria-Phage System



Antoni Luque, Chair
Department of Mathematics and Statistics



Ricardo Carretero
Department of Mathematics and Statistics



Forest Rohwer
Department of Biology

June 21 / 2017

Approval Date

Copyright © 2017
by
Emily Ann Jasien

DEDICATION

To my parents.

ABSTRACT OF THE THESIS

Modeling the Transition
Between Lytic and Lysogenic Behavior
in a Bacteria-Phage System

by

Emily Ann Jasien

Master of Science in Applied Mathematics with a Concentration in Dynamical Systems
San Diego State University, 2017

Phages are viruses that infect bacteria and exploit the bacterial metabolism to replicate. The ecological impact of phages is far reaching, and includes such mechanisms as the control of bacterial abundance and the promotion of nutrient turnover in environments. A recent study of microbial and viral abundances across ecosystems was conducted and published in Knowles *et al.* (Nature 2016). In this work, it was observed that as the abundance of microbes in ecosystems increased, the virus to microbe ratio decreased. This trend was proposed to correspond to an emergence of lysogeny, in which phages integrate their genome into the bacteria. A Piggyback-the-Winner model was suggested to describe these observed dynamics, instead of the established Kill-the-Winner model. In this thesis we have used dynamical systems to describe the bacteria-phage system and to explore the dynamics of the two models. We propose a mathematical model that incorporates lysogeny into bacteria-phage communities as a result of excess energy resources. This model predicts bacteria and phage equilibrium concentrations that align with the environmental observations and recovers qualitative trends from the data. Based on these results we propose a speciation model that includes both the dynamics of the Piggyback-the-Winner and Kill-the-Winner models as a way to promote the evolution of new species. Our model provides an interpretation of the observed dynamics of bacteria-phage interactions across ecosystems and leads to specific predictions that can be tested to validate these theoretical results.

TABLE OF CONTENTS

	PAGE
ABSTRACT	v
LIST OF TABLES.....	viii
LIST OF FIGURES	ix
ACKNOWLEDGMENTS	x
CHAPTER	
1 INTRODUCTION	1
1.1 Purpose	5
1.2 Format of the Thesis	6
2 LYTIC AND LYSOGENIC WORLDS	7
2.1 Lytic World: Single Species Model	7
2.2 Lysogenic World: Single Species Model.....	10
2.3 Combining the Lytic and Lysogenic Worlds	14
3 MIXED WORLDS INCLUDING BOTH VIRULENT AND TEMPER- ATE PHAGES	19
3.1 Temperate Phages Choose Lytic Lifestyle	19
3.2 Temperate Phages Choose Lysogenic Lifestyle	22
3.3 Temperate Phages have Lifestyle Decision	26
3.4 Virulent Phages able to Infect Lysogens	27
4 COMMUNITY WORLDS	31
4.1 Lytic World: Community Model	31
4.2 Lysogenic World: Community Model.....	35
4.3 Combining the Lytic and Lysogenic Community Worlds	37
4.4 A Proposed Speciation Model	38
5 CONCLUSIONS AND FUTURE WORK	41
BIBLIOGRAPHY	43
APPENDICES	
A BACKGROUND MATHEMATICS.....	46
B LYTIC AND LYSOGENIC WORLDS	49

C	MIXED WORLDS INCLUDING BOTH VIRULENT AND TEMPERATE PHAGES	57
D	COMMUNITY WORLDS	66
E	LATIN HYPERCUBE SAMPLING	77

LIST OF TABLES

	PAGE
Table 2.1. Meanings of Parameters Included in the Lytic World Model (Equation (2.1)) ..	8
Table 2.2. Meanings of Parameters Included in the Lysogenic World Model (Equation (2.6))	12
Table 3.1. Meanings of Parameters Included in the Mixed World Models	19
Table 3.2. Approximate Expressions of Equations (3.5)–(3.8) for different val- ues of K	25
Table 4.1. Meaning of Parameters Included in the Lytic World Community Model (Equation (4.1))	32
Table 4.2. Meaning of Parameters Included in the Lysogenic Community World Model (Equation (4.9))	36
Table B.1. Summary of the Stability of All Equilibrium Points in the Lytic World Model	53
Table B.2. Summary of the Stability of All Equilibrium Points in the Lysogenic World Model	55
Table E.1. Baseline Parameter Values Used in Latin Hypercube Sampling	78

LIST OF FIGURES

	PAGE
Figure 1.1. Visualization of the processes of lytic and lysogenic replication.	2
Figure 1.2. Viral particles vs. number of microbes across different ecosystems.	4
Figure 2.1. Impact of carrying capacity in the lytic world.	9
Figure 2.2. Effect of immunity in the lysogenic world.	13
Figure 2.3. Impact of carrying capacity on the lysogenic world.	14
Figure 2.4. Environmental data across ecosystems	15
Figure 2.5. Predicted environmental bacteria and phage concentrations from sampling the lytic and lysogenic worlds.	16
Figure 2.6. Predicted environmental bacteria and phage concentrations from a combination of the lytic and lysogenic worlds.	18
Figure 3.1. Impact of carrying capacity on a mixed world in which temperate phages always choose lytic replication.	21
Figure 3.2. Impact of carrying capacity on a mixed world in which temperate phages always choose lysogenic replication.	23
Figure 3.3. Effect of the lytic-lysogenic decision on the dynamics of a mixed model	27
Figure 3.4. Effect of the infection of lysogens by virulent phages on the dynam- ics of a mixed model.	28
Figure 4.1. Impact of the number of species in the lytic world community.	33
Figure 4.2. Impact of the number of species on the fraction of surviving phage communities	35
Figure 4.3. Predicted bacteria and phage concentrations from the combination of the lytic and lysogenic community worlds compared to environmental data.	39
Figure D.1. Kernel probability distributions from simulations of the lytic world community	71
Figure D.2. Kernel probability distributions from simulations of the lysogenic world community	75

ACKNOWLEDGMENTS

I would like to thank Dr. Luque for giving me the opportunity to work on this project, and providing support every step of the way. I would also like to thank my other committee members, Dr. Carretero and Dr. Rowher, for being a part of this process. The Viral Information Institute at SDSU has been an integral part of the progression of this research, and I thank each and every member who volunteered their time and expertise.

Lastly, I would like to thank the people in my life who have given me the love and support that got me to where I am today. My parents showed me that getting a good education is the best thing a person can do for themselves, and gave me the tools to succeed. Jason Thoma always encouraged me to persevere, even when things seemed impossible. This thesis would not exist without them.

CHAPTER 1

INTRODUCTION

Discovery and Importance of Phages. A virus is a microscopic organism that requires a living host cell to reproduce. While different viruses may have different specific structures, every virus is made up of proteins and genetic material, which is either RNA or DNA. Their genetic material is enclosed in a layer of proteins called a capsid. Though viruses are often associated with the infection of plant, animal, and human cells, their host range extends beyond this. Viruses also possess the ability to infect bacteria cells. F. W. Twort was the first to observe evidence of viral infection of bacteria in 1915. The bacteria he was studying were spontaneously destroyed, which he attributed to the effect of an enzyme. Felix d'Hérelle also witnessed the lysis of bacteria while conducting unrelated research two years later. He correctly concluded that this phenomenon was caused by an organism, and named it a bacteriophage, meaning “bacteria eater.” [35]. d'Hérelle recognized the potential to utilize these bacteriophages, or phages, to treat harmful diseases caused by bacteria. His findings led to the first explorations into the field of phage therapy. However, the success of antibiotics eventually caused many to abandon the idea of using phages to fight disease [24].

The nature of phages provided a way to answer many open biological questions. The quick turnover of phage populations lead to experimental evidence that mutations were present in bacteria without selection by Joshua and Ester Lederberg in 1952 [27]. The same year, Alfred Hershey and Martha Chase used the simple structure of phages to show that genetic material was made up of DNA. The first single-stranded DNA sequenced was that of phage ϕ X174 in 1977, and the first double-stranded DNA sequenced was that of phage λ in 1982 [24]. In 1989 counts of viruses in natural waters were found to be 10^3 - 10^7 times higher than previous estimates [1]. These findings illustrated that the interactions of microbes and phages could have a huge impact on the food web and the cycling of nutrients in an environment [3, 14]. The important role that phages play in microbial ecosystems has implications about their effect on the human microbiome. For example, the developing resistance of bacteria to antibiotics has initiated a renewed interest in the field of phage therapy.

Phage Lifestyle. Phage replication relies entirely on a successful encounter with a host bacterium. Without such an encounter a phage will eventually deactivate, which equates to the death of the phage. This may occur through the spontaneous destabilization of their structure, or from the effect of environmental factors, such as UV exposure [7, 35]. Phages

lack the ability to move themselves and rely on diffusion to navigate through the environment. When a phage comes in contact with a bacterium it may infect the bacterium by injecting its genetic material into the cell. There are then two possible types of replication: lytic or lysogenic. Figure 1.1 illustrates the difference between lytic and lysogenic replication.

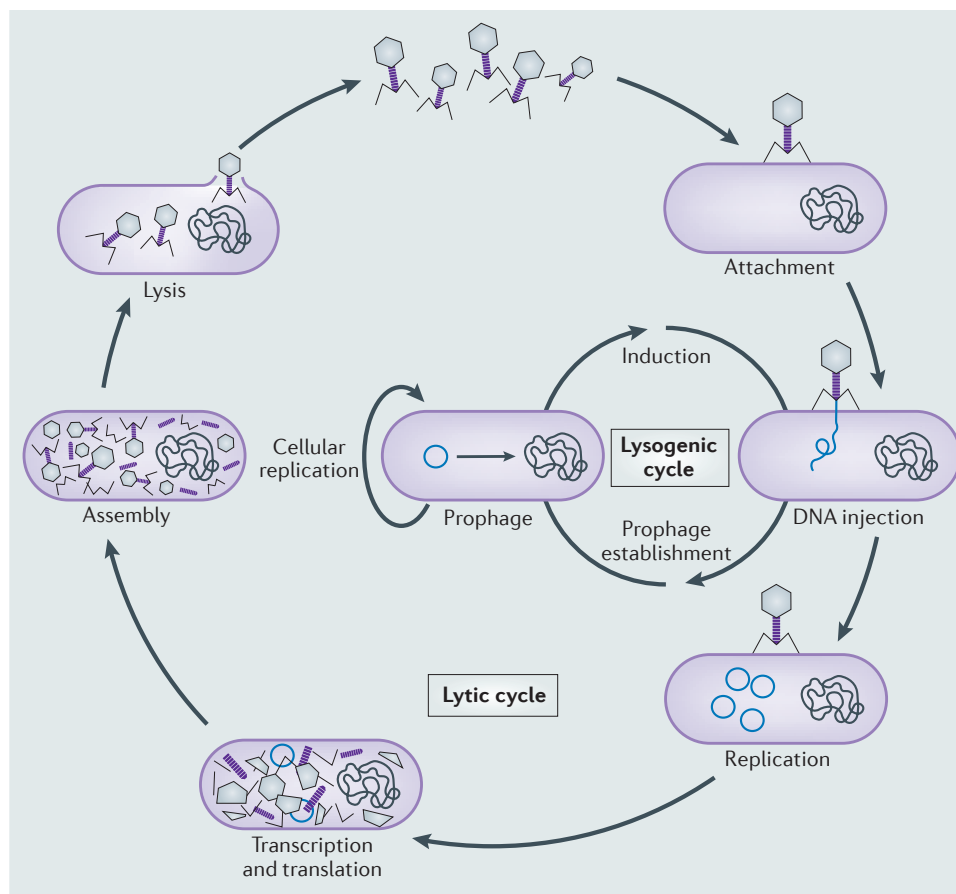


Figure 1.1. Visualization of the processes of lytic and lysogenic replication. Source: G. P. C. Salmond and P. C. Fineran, *A century of the phage: Past, present, and future*, Nature Reviews Microbiology, 13 (2015), pp. 779.

In lytic replication, an infection causes the bacterium to replicate the phage DNA and produce necessary components for the assembly of new virions, i.e., new infective viral particles. After the completion of this process, the bacteria lyses, releasing the phages into the environment [35]. In lysogenic replication, the phage's genetic material is integrated into the chromosome of the bacteria. This genetic material is then referred to as a prophage and the bacterium is referred to as a lysogen. The prophage is passed to the lysogen's progeny during replication. The relationship between a lysogen and its prophage is often one of symbiosis. Prophages can alter the phenotype of the bacterium, which may benefit the lysogen. This

lysogenic conversion will ultimately benefit the prophage because its survival is tied to the survival of its host [16]. For example, a prophage can give a lysogen immunity from infection by phages of the same or related strain [6]. The prophage maintains the ability to initiate lytic replication while integrated in the lysogen. This switch can occur spontaneously, or can be initiated by the bacteria's stress response to an environmental factor. Such factors include insufficient energy resources and UV exposure. The prophage elects to exit the cell in these circumstances as a form of self-preservation [35]. A lysogen may also be "cured" through the deactivation of its prophage by various mechanisms, such as mutation [6].

Based on their lifestyle, phages can be classified as either virulent or temperate. Virulent phages are restricted to lytic replication because they lack the necessary enzymes for integration. Temperate phages are able to choose between lytic or lysogenic replication. When a temperate phage chooses lysogenic replication and integrates into the chromosome of the host, it is referred to as prophage [35]. The ability of temperate phages to make a decision regarding their replication is a key idea for the work completed in this thesis.

Ecological Impact of Phage Lifestyle. The abundance of bacteria in an environment is believed to play an important role in the lifestyle decision of temperate phages. In environments with low abundances of bacteria, a lysogenic lifestyle would insure a higher chance of phage survival. In such systems the chance of an encounter between a phage and bacterium is assumed to be too low for successful lytic replication [21, 33]. In environments with high abundances of bacteria, the dynamics are predicted by a Kill-the-Winner (KtW) model [29, 35]. As the abundance of bacteria increases, it is assumed that the system can support phage production on a larger scale. Phages will then prefer lytic replication. In 2016 an alternate model was proposed, called Piggyback-the-Winner (PtW) [12]. This model contradicts KtW by predicting that as bacteria abundance increases, phages will transition from predominately lytic to lysogenic replication.

The Piggyback-the-Winner (PtW) model is based on an analysis of microbial and viral abundances across different ecosystems. A meta-analysis of data from 22 independent studies was completed and the results from [12] are given in Figure 1.2. One of the findings used to justify the PtW model is based on the trends of the virus to microbe ratio (VMR). VMR is a measurement of the number of viruses per microbe in the system. High VMRs are assumed to correspond to lytic behavior, while low VMRs are assumed to correspond to lysogenic behavior. The plot of the VMRs analyzed in [12] is given in the last row and last column of Figure 1.2. The data displays high VMR values for environments with mid-range microbial abundances, and low VMR values for environments with high microbial abundances. This suggests a transition from lytic to lysogenic dominance in the phage population as microbial abundance increases. Evidence that bacteria-phage dynamics are governed by a PtW model

was also found in the analysis of viral communities from 24 Pacific and Atlantic coral reefs. Communities with higher densities of microbes had an increased relative abundance of temperate viruses, which is an indication of lysogeny [12].

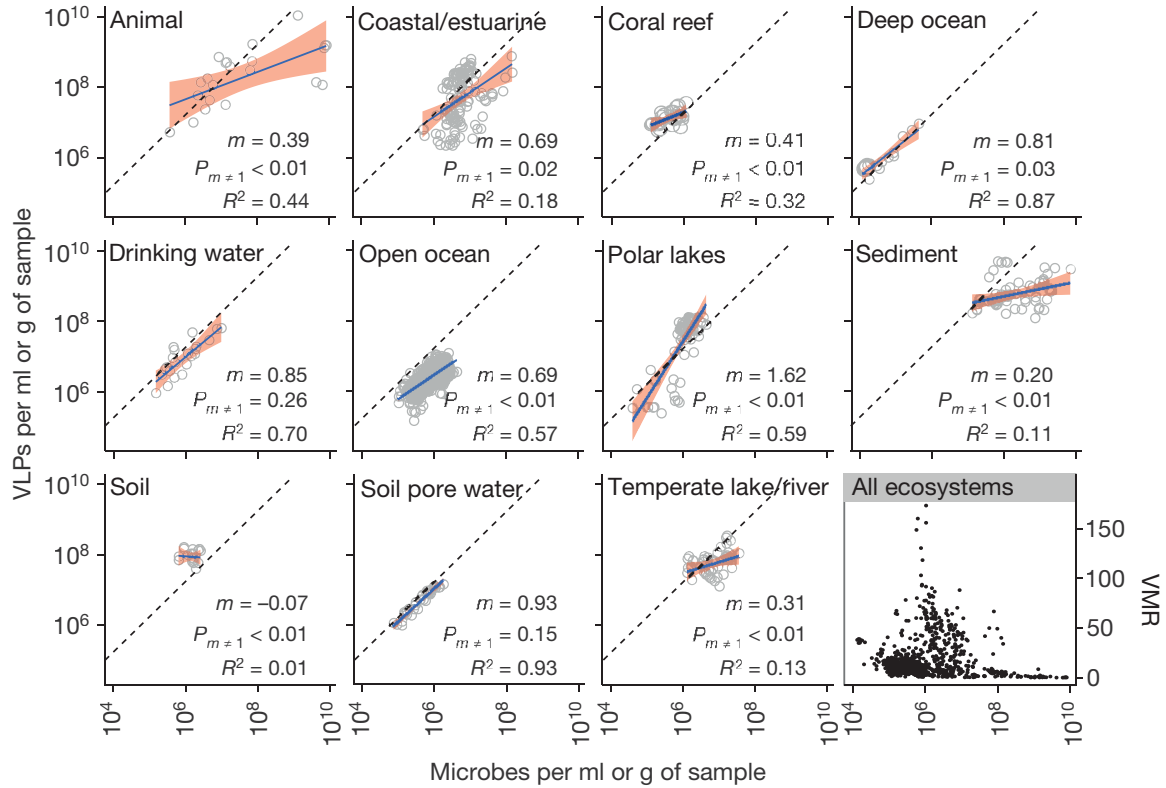


Figure 1.2. Viral particles vs. number of microbes across different ecosystems. In all panels excluding the last row and last column the solid line represents the linear regression of the log-transformed data, while the dotted line has a slope of one for reference. The panel in the last row and last column displays the virus to microbe ratios (VMRs) for all ecosystems as a function of microbial abundance. Source: B. Knowles et al., *Lytic to temperate switching of viral communities*, Nature, 531 (2016), pp. 468.

The ecological importance of the lifestyle of a phage implies that the predictions of the PtW model are extremely significant. Prophages can carry virulence factors that convert non-pathogenic bacteria to pathogenic lysogens. This awards the lysogens with protection, and can make these harmful bacteria extremely stable in an environment [4]. Thus, evidence of high amounts of lysogenic activity may indicate the condition of an ecosystem.

Coral reefs are one ecosystem that illustrates the importance of phage lifestyle. Phages exhibiting lytic replication can play a beneficial role in healthy reefs by controlling the abundance of bacteria [31]. When reefs are harmed by factors such as overfishing, this promotes an increase of algae in the ecosystem. Algae releases more dissolved organic carbon

(DOC) than corals. This DOC can be used by bacteria as a food source, thus it would be expected that an increase in algae would correspond to an increase in bacteria. Data from 60 different coral reef sites was analyzed and found that this prediction was valid in [10]. This analysis also indicated a possible positive relationship between the amount of algae in a reef and the abundance of virulence factors. Pathogenic bacteria can be detrimental to coral reefs, furthering the decline of these ecosystems and encouraging the growth of more algae. A large abundance of possibly pathogenic bacteria is indicative of lysogeny, according to the PtW model. Here, a switch in phage replication from lytic to lysogenic may indicate an extreme environmental shift in coral reefs.

Mathematical Models Incorporating Lytic and Lysogenic Replication.

Mathematical models that describe a physical system can be used to further the understanding of and make predictions about that system's dynamics. Many such models to study the dynamics of systems of bacteria and virulent phages have been proposed [9, 29, 35, 36]. However, models that also include populations of lysogens and temperate phages seem to be rare. The first such mathematical model was proposed by Stewart and Levin to study the lifestyle decision of temperate phages in 1984 [25]. In this model the authors include three bacteria populations: sensitive, lysogenic, and resistant. They also include a population of virulent phages, which only undergo lytic replication, and a population temperate phages, of which a fraction undergo lysogenic replication and the rest undergo lytic replication. Stewart and Levin use the analytical implications of their model to hypothesize why temperate phages would choose to become lysogenic. Only one simulation of their model is given and their results are not compared to environmental data. To the knowledge of the author there has been no subsequent models that follow the same vein as the one published in [25].

Other mathematical models of the bacteria-phage system that incorporate lysogeny include one proposed by Wang and Goldenfeld in 2010 [32]. Their model is an extension of that from [36] that includes a population of lysogens. In their analysis it is assumed that all phages are temperate and can choose lytic or lysogenic replication. Another similar model is discussed by Weitz and includes susceptible bacteria, lysogens, and phages that always choose lysogenic replication [35]. Neither model includes a population of virulent phages in the system.

It can be seen that there is a lack of mathematical models that describe a complete bacteria-phage system, which includes sensitive bacteria, virulent phages, lysogens, and temperate phages. This coupled with the evidence that a switch between a lytic and lysogenic dominated system plays a key role in ecosystems is the motivation for this thesis.

1.1 PURPOSE

The purpose of this thesis is to investigate mathematical models of the bacteria-phage system to understand the mechanisms behind environmental observations [12]. Throughout the analysis of the models the following question will be asked: Would phages benefit from a transition from lytic to lysogenic replication in this system? The results of this thesis are intended to be used to make predictions regarding the make-up and dynamics of bacteria-phage systems in the environment. These predictions will help biologists design new experiments to further the understanding of bacteria and phage ecology.

1.2 FORMAT OF THE THESIS

The main text of this thesis presents the results and biological implications from each model that was studied. The analysis of each model is given in the appendices with the necessary background mathematics given in Appendix A. Chapter 2 compares a lytic model and a lysogenic model. A combination of the models to interpret the trends of [12] is also presented. The detailed math analysis is given in Appendix B. Chapter 3 develops mixed models that incorporate both lytic and lysogenic replication and the mathematical details are included in Appendix C. Chapter 4 extends the lytic and lysogenic models discussed in Chapter 2 to their respective community models. These models are combined and compared to environmental data from [12]. Appendix D presents the detailed math analysis of the community models. Chapter 5 summarizes the results, predictions, and perspectives of the work completed in this thesis.

CHAPTER 2

LYTIC AND LYSOGENIC WORLDS

This chapter studies the dynamics of a bacteria-phage system in two extreme situations. The first is the lytic world, which consists of sensitive bacteria and phages that choose lytic replication. The second is the lysogenic world, which consists of lysogens that are spontaneously induced by their prophage, releasing phages into the system as a result. A comparison and combination of the two worlds is used to understand the underlying dynamics that regulate bacteria and phage abundance in the environment.

2.1 LYTIC WORLD: SINGLE SPECIES MODEL

A system consisting of one species of bacteria and one species of virulent phage is modeled. Each bacteria is susceptible to infection by phages, which choose lytic replication. The model is given by a system of two ordinary differential equations, one to describe the rate of change of the bacteria population and one to do the same for the phage population. Assuming that the populations are homogeneously mixed, the dynamics of the system are governed by the following mathematical model:

$$\begin{aligned} \frac{dM}{dt} &= \overbrace{r \left(1 - \frac{M}{K}\right) M}^{\text{logistic growth}} - \overbrace{dMV}^{\text{infection}}, \\ \frac{dV}{dt} &= \overbrace{cdMV}^{\text{lysis}} - \overbrace{mV}^{\text{decay}}. \end{aligned} \quad (2.1)$$

The bacteria population is represented by M and the phage population is represented by V . The population of bacteria grows logistically, which implies that it is limited by the population's carrying capacity, K . This growth is modeled by the first term in the rate of change equation for the bacteria population. The parameter r represents the intrinsic growth rate of M . When bacteria encounter a phage they are infected at a rate d . This interaction is described by the second term in the bacteria equation, which assumes the law of mass action. Infection leads to the lysis of the bacteria, releasing c phages into the system. The parameter c is referred to as the burst size of the phages. The process of lysis and viral release is assumed to be instantaneous and is modeled by the first term in the rate of change equation for the phage population. This model excludes a latent period between infection and viral release because the dynamics over long time scales are of interest here. Free phages are deactivated at

a rate m , which represents the decay rate of the phages. This mechanism is included in the model by the second term in the phage equation. All parameters are greater than zero and typical environmental values are given in Table 2.1.

Table 2.1. Meanings of Parameters Included in the Lytic World Model (Equation (2.1))

Parameter	Description	Value	Reference
r	intrinsic growth rate of bacteria	$1/24 \text{ hr}^{-1}$	[34]
K	carrying capacity of bacteria	$10^3\text{-}10^9 \text{ cells/ml}$	
d	infection rate of virulent phages	$10^{-8} \text{ ml/cells/hr}$	[34]
c	burst size of virulent phages	20 virons	[34]
m	decay rate of virulent phages	$1/6 \text{ hr}^{-1}$	[34]

The equilibrium populations of the model and the analysis of their stability is studied using standard techniques from the theory of dynamical systems (see Appendix B.1). A summary of the results are given in Table B.1.

In the lytic world, bacteria and phages are able to coexist in the system when the carrying capacity of the bacteria exceeds a threshold value, given by $K_0 = \frac{m}{cd}$. When $K < K_0$, the concentration of bacteria is too low for phages to produce enough new viral particles to overcome their decay rate. This leads to phage extinction, and in the absence of phages, the bacteria population grows to their carrying capacity, K . The system will stably remain at this bacteria-only equilibrium for $K < K_0$. This result implies that there is a minimum concentration of bacteria necessary for phages to survive in the system. Such a threshold has been observed experimentally in bacteria-phage interactions [38, 40].

At the threshold value, K_0 , a transcritical bifurcation occurs in the system, which elicits a transition in the dynamics. The bacteria-only equilibrium becomes unstable and the coexistence equilibrium becomes stable. When $K > K_0$, the carrying capacity of the system is large enough to allow coexistence between bacteria and phages. As the system moves to this state of coexistence, the concentrations of bacteria and phages oscillate with time. These oscillations decay until the system reaches equilibrium. In the lytic world, when an equilibrium is stable, it is globally stable. This implies that regardless of the initial concentrations of the system, when $K < K_0$ only bacteria will survive in the system and when $K > K_0$ there will be coexistence between the two populations (see Appendix B.1.2).

The equilibrium concentrations of bacteria, M^* , and phages, V^* , at coexistence are expressed in terms of parameters as follows:

$$M^* = \frac{m}{cd} = K_0, \quad (2.2)$$

$$V^* = \frac{r}{d} \left(1 - \frac{M^*}{K} \right) \sim \frac{r}{d}. \quad (2.3)$$

The equilibrium concentration of the bacteria is determined by the three phage parameters in the model: m , the decay rate, c , the burst size, and d , the infection rate. This implies that there is top-down control in this system, which is common in many predator-prey interactions. Here the phages are the predators which determine the size of the bacteria population, their prey [17]. The phage concentration saturates for large values of carrying capacity, i.e., $K_0/K \ll 1$. V^* is then a constant value of r/d in the asymptotic limit, indicated in Equation (2.3). This result implies that a lytic lifestyle can restrict the abundance of phages in systems with large carrying capacities.

The results from this model can serve as a valuable source of predictions in the analysis of environmental phage-bacteria data. To visualize these results the bacteria and phage concentrations are plotted as a function of carrying capacity in Figure 2.1 (a).

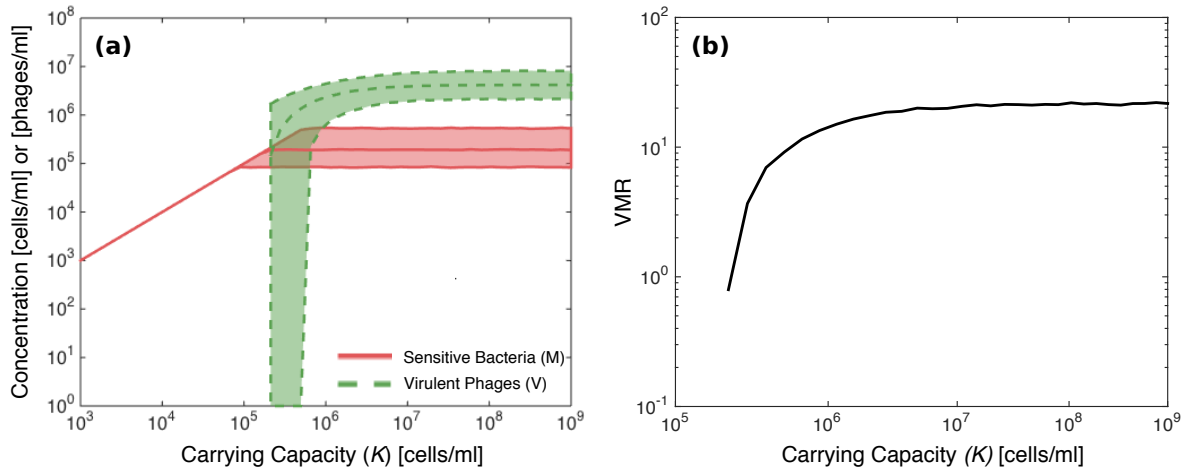


Figure 2.1. Impact of carrying capacity in the lytic world. (a) The equilibrium concentrations of bacteria and phages as a function of the carrying capacity. For each value of K , 10^4 relevant environmental parameter combinations were sampled using LHS (Appendix E). The middle line corresponds to the median, while the upper and lower bounds correspond to the 25th and 75th percentiles, respectively. (b) Virus to microbe ratio (VMR) as a function of the carrying capacity. The solid line corresponds to the median of the sampling and is plotted for carrying capacities that result in coexistence.

The variability in environmental parameters included in this model is simulated using a Latin Hypercube Sampling Scheme (Appendix E) with baseline values given in Table 2.1. From the sampling, the transition value is $K_0 \approx 10^5$ - 10^6 cells/ml. For carrying capacities lower than this value the bacteria are the only population in the system and grow to K with no variability. When the carrying capacity exceeds K_0 , this transition results in extreme variability in the phage population. Depending on the parameter sample, phages either enter the system at a high population or remain extinct during this transition. This leads to corresponding

variability in the bacteria population. After this transition, the bacteria and phage populations stabilize and the sampling leads to a constant variability. The constant values of the bacteria population lead to saturation in the phage population, which agrees with the asymptotic limit of $V^* \sim r/d$.

The virus to microbe ratio (VMR) is a common magnitude reported in environmental studies. Thus, it is important to analyze it for this model. At coexistence, the VMR of the lytic world is given in terms of parameters as follows:

$$\text{VMR} = \frac{rc}{m} \left(1 - \frac{m}{cdK} \right). \quad (2.4)$$

Figure 2.1 (b) plot the median of this quantity from the sampling as a function of carrying capacity. Using the asymptotic limit for V^* , Equation (2.4) can be written as follows:

$$\text{VMR} \sim \frac{rc}{m} \approx 5. \quad (2.5)$$

Thus, the model predicts that the phage decay rate, phage burst size, and bacteria intrinsic growth rate determine the ratio of phages and bacteria in the system. Using the magnitudes of baseline parameter values given in Table 2.1, the VMR is on the order of 5, which is in qualitative agreement with the typical observational values, $\text{VMR} \sim 10$ [12, 20]. The initial growth in the VMR observed in Figure 2.1 (b) corresponds to the transition from phage extinction to coexistence in the system.

The analysis of the lytic world reveals several characteristics of bacteria-phage systems that have been observed environmentally, such as typical virus to microbe ratios. The top-down control by the phages leads to saturation in the system, which leaves a portion of the energy resources unused. These available resources could then facilitate the invasion of other bacteria and phages into the system. This observation is relevant given the dynamics of lysogenic world discussed in the next section.

2.2 LYSOGENIC WORLD: SINGLE SPECIES MODEL

A system consisting of one species of lysogens and one species of temperate phages is modeled. Each lysogen contains phage DNA in the form of a prophage, which may spontaneously induce the bacteria to lyse and release temperate phages into the system. The dynamics of this system are described by a system of two ordinary differential equations, one to describe the rate of change of the population of lysogens and one to do the same for the phage population. The mathematical model is based on the assumption that the populations are homogeneously mixed and is given below:

$$\begin{aligned}
\frac{dL}{dt} &= \overbrace{r \left(1 - \frac{L}{K}\right) L}^{\text{logistic growth}} - \overbrace{\beta L}^{\text{induction}}, \\
\frac{dT}{dt} &= \overbrace{c\beta L}^{\text{lysis}} - \overbrace{mT}^{\text{decay}} - \overbrace{\chi dLT}^{\text{immunity of } L}.
\end{aligned} \tag{2.6}$$

In this model the lysogen population is represented by L and the phage population is represented by T . The lysogen population grows logistically, implying that it is limited by the carrying capacity of the population, K . This growth is captured by the first term in the equation representing the rate of change of the lysogen population. The parameter r represents the intrinsic growth rate of L . Note that when lysogens replicate they always produce lysogen progeny. Prophages spontaneously enter the lytic replication cycle and induce lysis of the lysogen at a rate β . This process is independent of interactions with the free phages in the system, and is described by the second term in the lysogen equation. This lysis releases c free phages, corresponding to the first term in the equation describing the rate of change of the phage population. Just as in the lytic world model (Equation (2.1)), c represents the burst size of the phages and m represents their decay rate. Phage decay is given by the second term in the phage equation. Lysogens are assumed to be immune to infection by temperate phages. This immunity can correspond to two different types of protection which determine the result of an encounter between a lysogen and a phage. Internal protection implies that the phage is able to enter the lysogen and is then deactivated. External protection implies that the phage does not attempt to infect the lysogen and is unaffected by the encounter. The lysogen population may exhibit a mixture of these types of protection, represented by the parameter $\chi \in [0, 1]$. A value of $\chi = 0$ implies that the protection is purely external and $\chi = 1$ implies it is purely internal. This mechanism is described by the last term in the phage equation, which assumes that encounters are determined by the law of mass action. All parameters excluding χ are always greater than zero and typical environmental values are given in Table 2.2.

The equilibrium populations of the model and the analysis of their stability is studied using standard techniques from the theory of dynamical systems (see Appendix B.2). A summary of these results are given in Table B.2.

In the lysogenic world, lysogens and phages coexist when the intrinsic growth rate of the lysogens is faster than the induction rate of the prophages, i.e., $r > \beta$. When this condition is not met, the lysogens are lysed more often than they replicate, resulting in the extinction of both populations. From Table 2.2, it is clear that the spontaneous induction rate is generally many magnitudes smaller than the growth rate of the lysogens, i.e., $r \gg \beta$ [2]. The coexistence equilibrium is globally stable, which implies that regardless of the initial

Table 2.2. Meanings of Parameters Included in the Lysogenic World Model (Equation (2.6))

Parameter	Description	Value	Reference
r	intrinsic growth rate of lysogens	$1/24 \text{ hr}^{-1}$	[34]
K	carrying capacity of lysogens	$10^3\text{-}10^9 \text{ cells/ml}$	
β	spontaneous induction rate of prophage	$(1/24) \times 10^{-6} \text{ hr}^{-1}$	[22, 23]
c	burst size of temperate phage	20 virons	[34]
m	decay rate of temperate phage	$1/6 \text{ hr}^{-1}$	[34]
d	infection rate of temperate phage	$10^{-8} \text{ ml/cells/hr}$	[34]
χ	type of lysogen immunity	in the range $[0, 1]$	

concentrations of the system, lysogens and temperate phages will always coexist (see Appendix B.2.2).

The equilibrium concentrations at coexistence of lysogens, L^* , and temperate phages, T^* , are expressed in terms of parameters as follows:

$$L^* = \left(1 - \frac{\beta}{r}\right) K \approx K, \quad (2.7)$$

$$T^* = \frac{c\beta L^*}{m + \chi d L^*} \approx \frac{c\beta K}{m + \chi d K}. \quad (2.8)$$

The equilibrium population of lysogens grows linearly with the carrying capacity, K . The fact that $r \gg \beta$ reveals that the expression of L^* is approximately K , indicated in Equation (2.7). In this system the lysogens are able to use nearly all of the energy resources available to them.

The type of lysogen immunity, given by χ , determines the value of T^* , which is illustrated in Figure 2.2 (a). When the protection of the lysogens is purely external ($\chi = 0$) Equation (2.8) is approximately

$$T^* \approx \frac{c\beta}{m} K. \quad (2.9)$$

Here the phage population grows linearly with the carrying capacity because more free phage are able to remain in the environment. For all other values of χ the temperate phage population undergoes a transition from linear growth with K to saturation in the system. The value of K that determines this transition is found to be

$$\bar{K} \approx 10^n, \quad (2.10)$$

where $n \approx 7 + y$ and $\chi = 10^{-y}$ (see Appendix B.2.3). This expression shows that as the amount of internal protection of the lysogens increases (χ becomes larger) the temperate phage population saturates in the system for smaller values of \bar{K} . In Figure 2.2 (a) as the value of χ increases the curve deviates from linear growth at smaller values of \bar{K} , as predicted.

The virus to microbe ratio (VMR) for this system is given by the following expression:

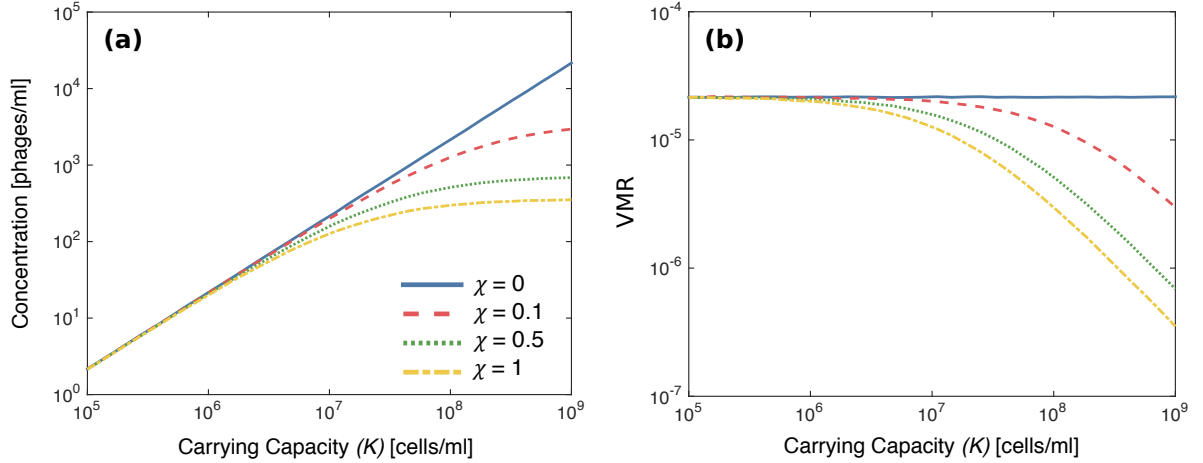


Figure 2.2. Effect of immunity in the lysogenic world. (a) The equilibrium concentration of temperate phages for different values of χ as a function of the carrying capacity. For each value of K , 5×10^4 relevant environmental parameter combinations were sampled using LHS (Appendix E). (b) Virus to microbe ratio (VMR) for different values of χ as a function of the carrying capacity. Both panels plot the median of the sampling.

$$\text{VMR} = \frac{c\beta}{m + \chi dL^*} \approx \frac{c\beta}{m + \chi dK}. \quad (2.11)$$

The transition in the behavior of T^* determines a corresponding transition in the VMR of the system. For $K < \bar{K}$ the VMR is constant, but once $K > \bar{K}$ it tends to zero. This behavior is displayed in Figure 2.2 (b).

The lysogen and phage populations are plotted as a function of carrying capacity in Figure 2.3 (a). The variability in environmental parameters is simulated using a Latin Hypercube Sampling Scheme (Appendix E), with baseline values given in Table 2.2. For all values of K the lysogen population appears to be near carrying capacity, as predicted by the approximation for L^* . The qualitative behavior of T^* remains the same for $\chi > 0$, thus $\chi = 0.5$ is chosen for this plot.

The VMR values of the lysogenic world are extremely low which would seem to imply that choosing a lysogenic lifestyle leaves phages at a disadvantage. However, recall that each lysogen contains a prophage with the ability to enter the lytic cycle. In Figure 2.3 (b) the median prophage to microbe ratio (PMR) and median VMR values are shown as functions of K . Each lysogen contains a prophage, making the PMR one for all values of K . Thus, while the number of free phages in the system is low compared to the number of lysogens, phage genomes remain at comparable numbers to lysogen genomes in the system.

The analysis of the lysogenic world indicates that lysogens are extremely stable as a result of the very low induction rate of the prophages. This agrees with observations from the study of lysogeny [22]. The ability of lysogens to utilize almost all of the available energy

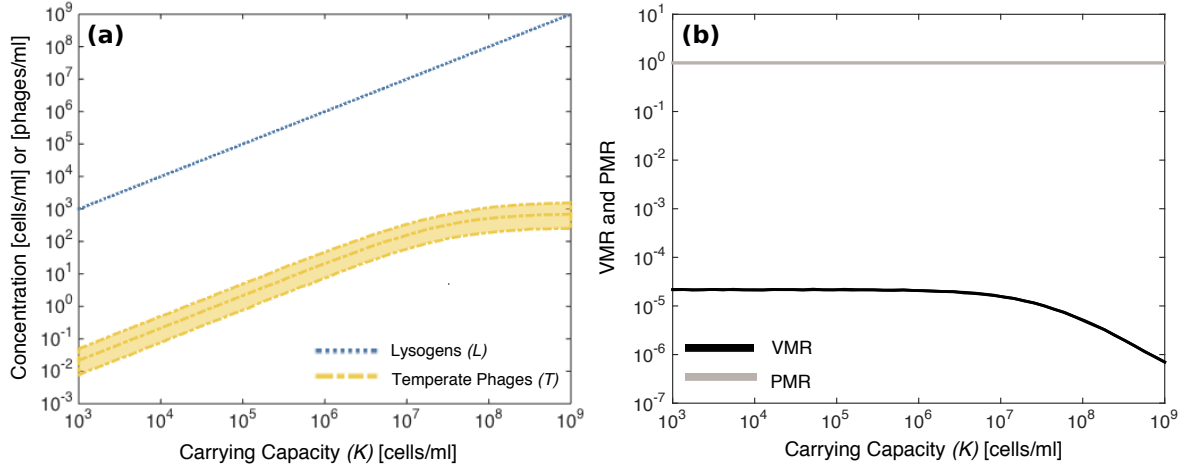


Figure 2.3. Impact of carrying capacity on the lysogenic world. (a) The equilibrium concentrations of lysogens (blue) and temperate phages (yellow) as a function of the carrying capacity with $\chi = 0.5$. For each value of K , 10^4 relevant environmental parameter combinations were sampled using LHS (Appendix E). The middle line corresponds to the median, while the upper and lower bounds correspond to the 25th and 75th percentiles, respectively. (b) Prophage to microbe ratio (PMR) (grey) and median virus to microbe Ratio (VMR) (black) as a function of carrying capacity.

resources in the system demonstrates a possible interaction with the lytic world. Lysogens may be able to invade lytic-dominated systems and take advantage of the system's unused energy resources. This observation justifies the study of a combination of the lytic and lysogenic worlds discussed in the next section.

2.3 COMBINING THE LYTIC AND LYSOGENIC WORLDS

The results presented in Sections 2.1 and 2.2 provide an understanding of the lytic and lysogenic worlds as separate systems. A more complete picture of bacteria-phage dynamics requires a combination of the worlds. This is made apparent from a comparison of the lytic and lysogenic worlds to the environmental bacteria-phage data from [12]. The data is taken from 22 independent studies which include samples from a variety of different ecosystems (see Figure 1.2). A plot of the data is given in Figure 2.4. Panel (a) displays the concentration of virus-like particles (VLPs) as a function of the microbe concentration. The corresponding VMRs are plotted as a function of the microbe concentration in panel (b). Here Piggyback-the-Winner dynamics are observed; as the microbe concentration increases, the VMR decreases.

The predictions of the lytic and lysogenic worlds are compared to Figure 2.4 by a sampling over the parameter space for each world. This is completed using a Latin Hypercube

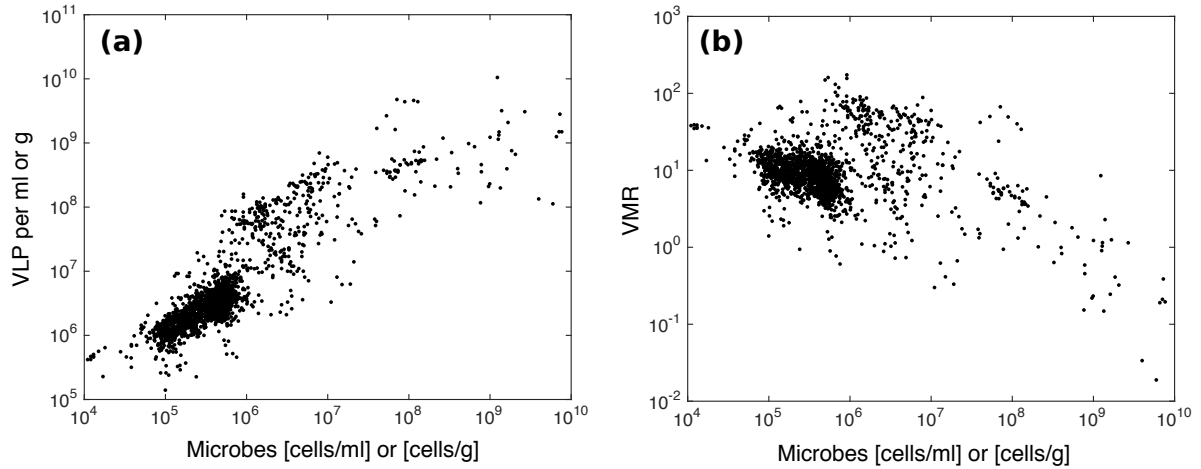


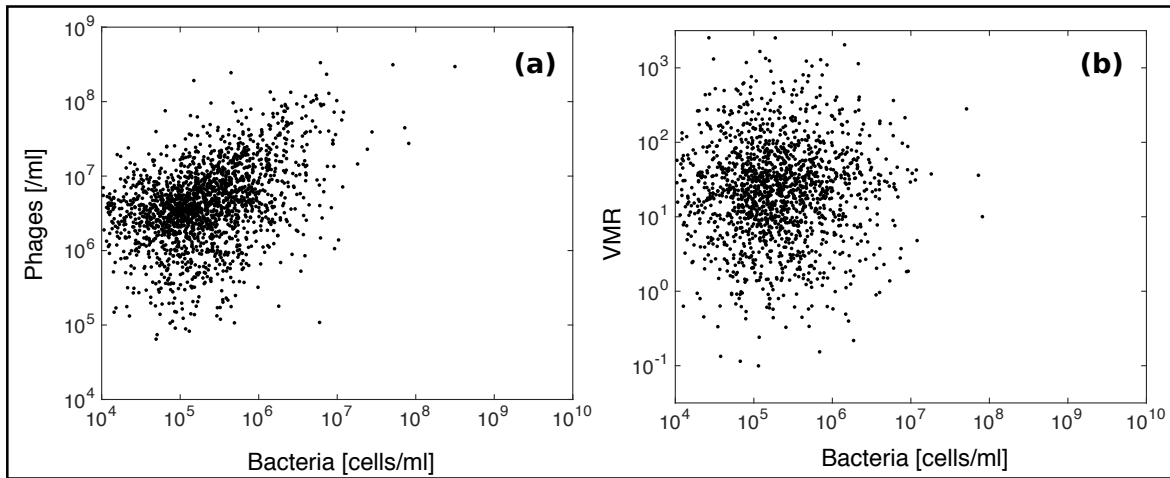
Figure 2.4. Environmental data across ecosystems. (a) Concentration of virus-like particles (VLPs) as a function of microbe concentration. (b) Virus to microbe ratio (VMR) as a function of microbe concentration. Data source: B. Knowles et al., *Lytic to temperate switching of viral communities*, Nature, 531 (2016), pp. 466–470.

Sampling Scheme (see Appendix E). Here the carrying capacity of the system is treated as a parameter. The samples are used to calculate 2000 stable, coexisting pairs of bacteria and phage concentrations for each world. Figure 2.5 (a) displays the concentration of phages as a function of the bacteria concentration in the lytic world. Panel (b) displays the corresponding VMRs as a function of the bacteria concentration. For the lysogenic world panel (c) displays the phage concentrations and (d) displays the VMRs, both plotted as a function of the bacteria concentration.

In the lytic world, top-down control restricts the concentrations that the bacteria can reach in the system. This results in a cloud of points for bacteria concentrations ranging from approximately 10^4 - 10^7 cells/ml in Figure 2.5 (a). In Figure 2.4 (a) a similar cloud of points is observed in the data for this range of microbe concentrations. Both clouds correspond to virus concentrations of approximately 10^5 - 10^8 phages/ml. This would suggest that the densest region of points in Figure 2.4 (a) is consistent with a dominance of lytic behavior in the virus population. The VMRs for the lytic world given in Figure 2.5 (b) do not display a discernible trend of either increase or decrease.

In the lysogenic world, there are no limitations on the size of the lysogen population in the system, as observed in Figure 2.5 (c). It was found in Section 2.2 that the lysogen population is able to attain values extremely close to their carrying capacity. Thus, the trends seen here are those discussed in Section 2.2. Of interest is the saturation in the phage concentrations at large bacteria concentrations. In Figure 2.4 (a), the environmental data displays a similar leveling off of the viruses for microbe concentrations in the range of

Lytic World



Lysogenic World

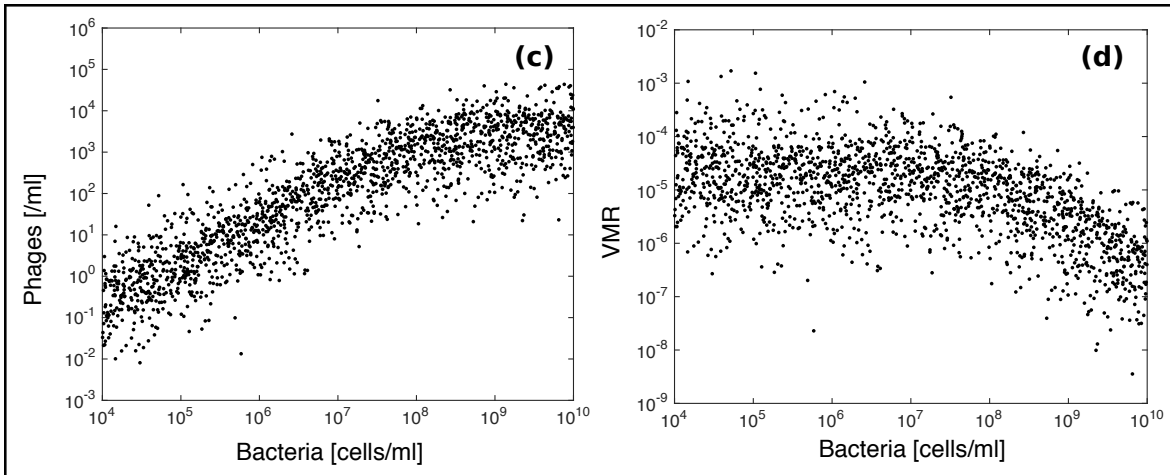


Figure 2.5. Predicted environmental bacteria and phage concentrations from sampling the lytic and lysogenic worlds. (a) Concentration of phages as a function of bacteria concentration in the lytic world. (b) Virus to microbe ratio (VMR) as a function of bacteria concentration in the lytic world. (c) Concentration of phages as a function of bacteria concentration in the lysogenic world. (d) Virus to microbe ratio (VMR) as a function of bacteria concentration in the lysogenic world. Data used in each panel was generated by calculating the stable bacteria and phage concentrations from each model using 2000 relevant environmental parameter combinations created from LHS (Appendix E).

10^8 - 10^{10} cells/ml or cells/g. It would be predicted that viruses choose lysogenic replication in this region. Note, however, that the phage concentrations and VMRs in the lysogenic world remain at much lower values than the environmental data.

From this comparison it is clear that neither the lytic nor the lysogenic world alone recreate the observed trends in the environmental data. Each world does however display certain characteristics present in Figure 2.4. This leads to the study of a compartmental model including both the lytic and lysogenic worlds. In this model each data point from the sampling is assumed to be made up of a combination of the two systems. As previously discussed, in the lytic world the top-down control of the phages prevents the bacteria from utilizing all of the available energy resources. The unused resources could then be accessed by lysogens, as they are not restricted by any such control. This interaction of the two worlds determines the combination scheme to be used. For each parameter sample the stable coexisting bacteria and phage populations from the lytic world are calculated. It is then assumed that a fraction of the remaining energy resources in the system can be utilized by the lysogenic world. This was implemented by creating 2000 points from the range 0-10% and assigning each value to a sample. This fraction depends on the total resources in the system and increases as the amount of resources increase [10, 18]. The values of K used in the sampling were ordered and each percentage assigned to simulate this. The total bacteria population is then made up of sensitive bacteria and lysogens and the total phage concentration is made up of virulent and temperate phages. For this system, the total phage concentration is plotted as a function of the total bacteria concentration in Figure 2.6 (a). The VMRs are plotted as a function of the total bacteria concentration in panel (b).

This combination of the lytic and lysogenic worlds recovers some of the trends observed in the environmental data. In Figure 2.6 (a) there is a cloud of points for low bacteria concentrations, and a leveling off of the phage concentrations for higher bacteria concentrations. The VMRs of the combination shown in Figure 2.6 (b) also decrease as bacteria concentration increases, as expected. There is however a discrepancy between the values that are obtained from the observational data and from the model combination. In Figure 2.4 (a) the virus concentrations reach values that are many magnitudes larger than what is seen in Figure 2.6 (a). This subsequently creates a discrepancy in the VMRs.

While the trends of the environmental data are not exactly reproduced by the combination, the compatibility of the dynamics is promising. These results lead to two methods to more accurately model this system. A compartmental model ignores the explicit interactions between the populations of the lytic and lysogenic worlds. It may be that these interactions are extremely important in the system. Chapter 3 explores the dynamics of mixed models that incorporate populations of sensitive bacteria, virulent phages, lysogens, and temperate phages. In the environment, a bacteria-phage system would be composed of many species. The lytic and lysogenic worlds only model single species systems, which may

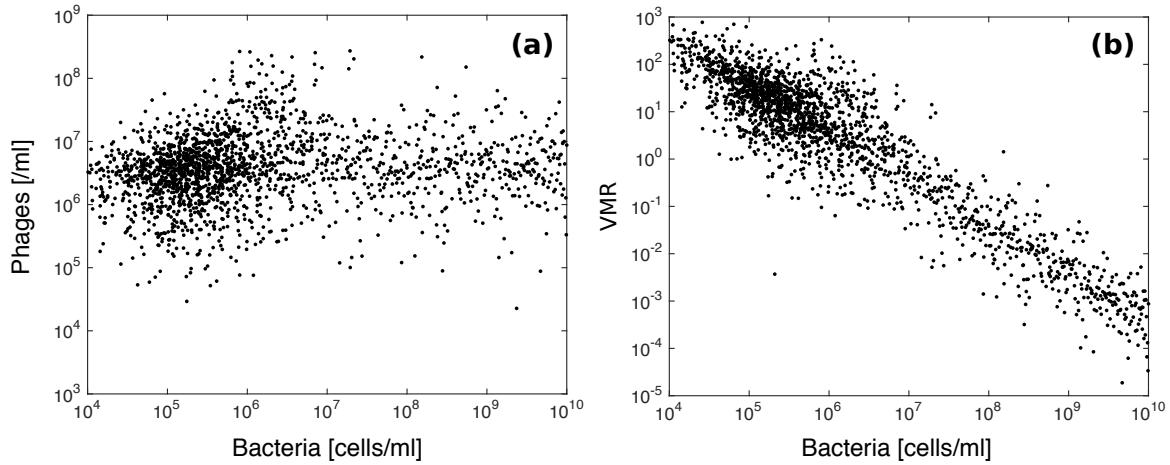


Figure 2.6. *Predicted environmental bacteria and phage concentrations from a combination of the lytic and lysogenic worlds.* (a) Concentration of phages as a function of bacteria concentration. (b) Virus to microbe ratio (VMR) as a function of bacteria concentration. Data was generated using 2000 relevant environmental parameter combinations created from LHS (Appendix E) and a combination scheme described in Section 2.3.

explain the discrepancy in the predicted concentrations and the data. Chapter 4 discusses the effect of extending the lytic and lysogenic worlds to community models.

CHAPTER 3

MIXED WORLDS INCLUDING BOTH VIRULENT AND TEMPERATE PHAGES

This chapter explores the dynamics of different bacteria-phage systems that include the direct interaction of sensitive bacteria, virulent phages, lysogens, and temperate phages. It begins with a discussion of a model in which temperate phages exclusively choose a lytic lifestyle (Section 3.1), which is followed by the discussion of a model in which temperate phages exclusively choose a lysogenic lifestyle (Section 3.2). The model will then be altered to allow temperate phages the freedom to choose either lifestyle (Section 3.3). The final model that is discussed is one in which a portion of the virulent phage population is able to infect lysogens (Section 3.4). The parameters used across all models and their typical values are given in Table 3.1.

Table 3.1. Meanings of Parameters Included in the Mixed World Models

Parameter	Description	Value	Reference
r	intrinsic growth rate of sensitive bacteria and lysogens	$1/24 \text{ hr}^{-1}$	[34]
K	carrying capacity of sensitive bacteria and lysogens	$10^3\text{-}10^9 \text{ cells/ml}$	
d	infection rate of virulent and temperate phages	$10^{-8} \text{ ml/cells/hr}$	[34]
c	burst size of virulent and temperate phages	20 virons	[34]
m	decay rate of virulent and temperate phages	$1/6 \text{ hr}^{-1}$	[34]
β	induction rate of prophage	$(1/24) \times 10^{-6} \text{ hr}^{-1}$	[22, 23]
s	curing rate of lysogens	$(1/24) \times 10^{-6} \text{ hr}^{-1}$	[11]
χ	immunity of lysogens	$[0, 1]$	

3.1 TEMPERATE PHAGES CHOOSE LYTIC LIFESTYLE

Temperate phages that exhibit lytic replication are modeled by prophages that immediately induce their host, i.e., $\beta \rightarrow \infty$. The absence of lysogens reduces the mixed world

to one consisting of sensitive bacteria, virulent phages, and temperate phages. Here each bacteria is susceptible to infection by both species of phage. The model is given by a system of three ordinary differential equations, one to describe the rate of change for each species in the system. The assumption that the populations are homogeneously mixed leads to the following mathematical model:

$$\begin{aligned}
 \frac{dM}{dt} &= \overbrace{r \left(1 - \frac{N}{K}\right) M}^{\text{logistic growth}} - \overbrace{dMV}^{\text{infection by } V} - \overbrace{dMT}^{\text{infection by } T}, \\
 \frac{dV}{dt} &= \overbrace{cdMV}^{\text{lysis}} - \overbrace{mV}^{\text{decay}}, \\
 \frac{dT}{dt} &= \overbrace{cdMT}^{\text{lysis}} - \overbrace{mT}^{\text{decay}}.
 \end{aligned} \tag{3.1}$$

The bacteria population is represented by M , the virulent phage population is represented by V , and the temperate phage population is represented by T . Interactions between bacteria and each species of phages are identical to those described in the lytic world (Section 2.1). Virulent and temperate phages are assumed to have identical parameter values and to have no direct interaction with each other. All parameters are always greater than zero and their typical values are given in Table 3.1.

The equilibrium populations of the model and the analysis of their stability is studied using standard techniques from the theory of dynamical systems (see Appendix C.1).

In terms of bacteria and total phage populations the system exhibits identical behavior to that of the lytic world. When the carrying capacity of the system is less than the threshold value, $K < K_0 = \frac{m}{cd}$, both phage species are unable to survive. This allows the bacteria population to grow to its carrying capacity, K . When $K > K_0$ the system transitions to a state of coexistence between all three populations. The equilibrium concentrations of bacteria, M^* , and total phages, $P^* = V^* + T^*$, are expressed in terms of parameters below:

$$M^* = \frac{m}{cd} = K_0, \tag{3.2}$$

$$P^* = \frac{r}{d} \left(1 - \frac{M^*}{K}\right) \sim \frac{r}{d}. \tag{3.3}$$

Figure 3.1 (a) displays the bacteria and total phage equilibrium concentrations as a function of the carrying capacity of the system. Panel (b) displays the virus to microbe ratio (VMR) as a function of carrying capacity. The variability in environmental parameters is simulated using a Latin Hypercube Sampling Scheme (Appendix E), with baseline values given in Table 3.1.

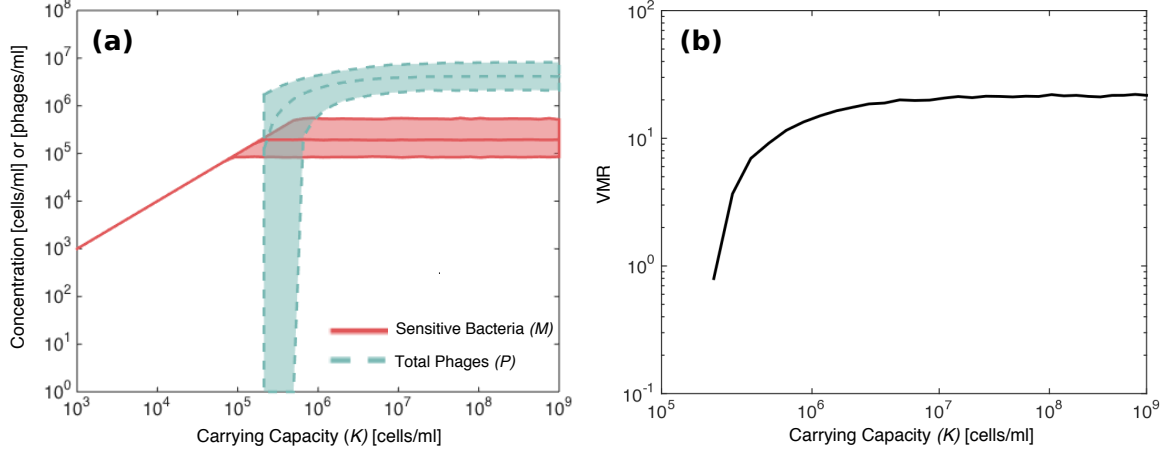


Figure 3.1. Impact of carrying capacity on a mixed world in which temperate phages always choose lytic behavior. (a) The equilibrium concentrations of bacteria (red) and total phages (turquoise) as a function of the carrying capacity. For each value of K , 10^4 relevant environmental parameter combinations were sampled using LHS (Appendix E). The middle line corresponds to the median, while the upper and lower bounds correspond to the 25th and 75th percentiles, respectively. (b) Virus to microbe ratio (VMR) as a function of the carrying capacity. The solid line corresponds to the median of the sampling and is plotted for carrying capacities that result in coexistence.

Though the plots given in Figure 3.1 appear identical to those from the lytic world (Figure 2.1), there are underlying dynamics at play in this system. Equation (3.3) gives the equilibrium concentration for the total phage population, P^* , but does not indicate the explicit values of V^* and T^* . Both species of phage compete for the same prey and are assumed to have identical properties. Therefore neither species has an advantage over the other, and the distribution of phage species will depend on the initial state of the system. Let V_0 be the initial concentration of virulent phages, T_0 be the initial concentration of temperate phages, and P_0 be the initial total phage concentration. For all $t \in [0, \infty)$ the following is true:

$$\frac{V(t)}{P(t)} = \frac{V_0}{P_0} \quad \text{and} \quad \frac{T(t)}{P(t)} = \frac{T_0}{P_0},$$

(see Appendix C.1). The distribution of the phage species remains the same for all time, giving the advantage to the species able to initially reach a higher population.

It is predicted that in a mixed world where all temperate phages choose lytic replication, the total phage population will saturate in the system. This behavior was observed in the dynamics of the lytic world (Section 2.1). Lytic replication prevents the phages from reaching higher populations, even in systems with large amounts of energy resources.

3.2 TEMPERATE PHAGES CHOOSE LYSOGENIC LIFESTYLE

An explicit population of lysogens is introduced into the mixed world when temperate phages exclusively choose lysogenic replication. Here the dynamics of the full system is modeled by a system of four ordinary differential equations, one to describe the rate of change of each of the four populations present. Assuming that the populations are homogeneously mixed, the mathematical model is given below:

$$\begin{aligned}
 \frac{dM}{dt} &= \overbrace{r \left(1 - \frac{N}{K}\right) M}^{\text{logistic growth}} - \overbrace{dMV}^{\text{infection by } V} - \overbrace{dMT}^{\text{infection by } T} + \overbrace{sL}^{\text{curing}}, \\
 \frac{dV}{dt} &= \overbrace{cdMV}^{\text{lysis}} - \overbrace{\chi dVL}^{\text{immunity of } L} - \overbrace{mV}^{\text{decay}}, \\
 \frac{dL}{dt} &= \overbrace{r \left(1 - \frac{N}{K}\right) L}^{\text{logistic growth}} - \overbrace{\beta L}^{\text{induction}} + \overbrace{dMT}^{\text{M infected by } T} - \overbrace{sL}^{\text{curing}}, \\
 \frac{dT}{dt} &= \overbrace{c\beta L}^{\text{lysis}} - \overbrace{\chi dTL}^{\text{immunity of } L} - \overbrace{dMT}^{\text{infection of } M} - \overbrace{mT}^{\text{decay}}.
 \end{aligned} \tag{3.4}$$

The bacteria population is represented by M , the virulent phage population is represented by V , the lysogen population is represented by L , and the temperate phage population is represented by T . Many of the interactions in this system are identical to those of the lytic and lysogenic worlds, thus only new interactions will be discussed. In this system the carrying capacity corresponds to the total bacteria population, represented by $N = M + L$. The logistic growth terms in the equations for the rate of change of both the sensitive bacteria and lysogens are changed accordingly. Sensitive bacteria are infected when they encounter either a virulent or temperate phage, given by the second and third terms in the bacteria equation, respectively. Infection by a temperate phage will result in the production of a lysogen. Lysogens can be “cured” from the prophage and return to the sensitive bacteria population at a rate s [35]. The result of a phage-lysogen encounter is again determined by the value of the parameter χ . It is assumed that the sensitive bacteria and lysogens have the same intrinsic growth rate, r , and that the burst size, c , infection rate, d , and decay rate, m , are the same for both virulent and temperate phages. All parameters excluding χ are always greater than zero and typical values are given in Table 3.1.

The equilibrium populations of the model and the analysis of their stability is studied using standard techniques from the theory of dynamical systems and numerical stability analysis (see Appendix C.2). The results of this analysis are used to plot the concentrations of

sensitive bacteria, virulent phages, lysogens, and temperate phages as a function of the carrying capacity in Figure 3.2 (a). The variability of the environmental parameters are simulated using a Latin Hypercube Sampling Scheme (Appendix E) with baseline values given in Table 3.1.

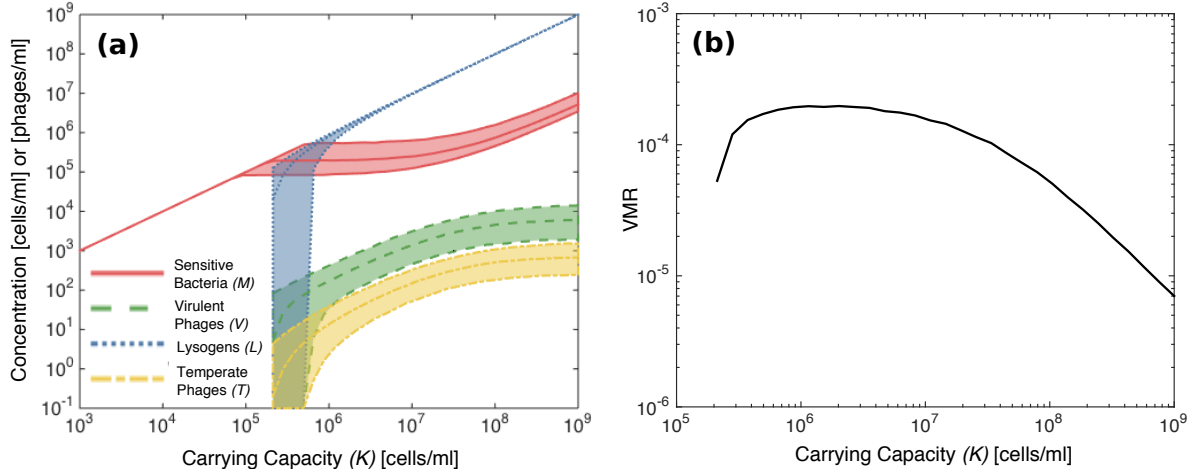


Figure 3.2. Impact of carrying capacity on a mixed world in which temperate phages always choose lysogenic replication. (a) The equilibrium concentrations of sensitive bacteria (red), virulent phages (green), lysogenic bacteria (blue), and temperate phages (yellow) as a function of the carrying capacity with $\chi = 0.5$. For each value of K , 10^4 relevant environmental parameter combinations were sampled using LHS (Appendix E). The middle line corresponds to the median, while the upper and lower bounds correspond to the 25th and 75th percentiles, respectively. (b) Virus to microbe ratio (VMR) as a function of the carrying capacity. The solid line corresponds to the median of the sampling and is plotted for carrying capacities that result in coexistence.

When the lysogens exhibit some internal immunity ($\chi > 0$) there are three distinct regions in which the system displays extremely different dynamics with respect to K . The first region corresponds to the values $0 < K < K_0$, where $K_0 = \frac{m}{cd}$. For these K values the system behaves similarly to that of the lytic world (Section 2.1). Neither species of phage are able to encounter a sensitive bacteria often enough to overcome their decay rate. In the absence of phages, lysogens and sensitive bacteria are left to compete for the system's energy resources. However, the spontaneous induction of the prophage puts the lysogens at a disadvantage that eventually results in their extinction. Thus only sensitive bacteria are able to survive and grow to carrying capacity in this region. This behavior can be observed in Figure 3.2 (a) for small values of K .

For $K > K_0$ there is a sufficient concentration of energy resources in the system to sustain coexistence between all four populations for most parameter samples. It should be

noted that the system occasionally has a stable equilibrium consisting of only sensitive bacteria, lysogens, and temperate phages, but this occurs rarely. Here, only the coexistence of all populations is discussed here. (see details in Appendix C.2.2).

The transition value K_0 is approximately 10^5 - 10^6 cells/ml from the sampling and corresponds to a large variability in the lysogen and phage populations observed in Figure 3.2 (a). Past this transition there is coexistence in the systems and the equilibrium concentrations of the four populations are given below:

$$M^* = \frac{m}{cd} + \frac{\chi}{c} L^*, \quad (3.5)$$

$$V^* = \frac{r}{d} \left(1 - \frac{N^*}{K} \right) + \frac{s}{d} \frac{L^*}{M^*} - T^*, \quad (3.6)$$

$$L^* = \frac{c}{c + \chi} \left(\left(1 - \frac{\beta}{r(1+c)} - \frac{s}{r} \right) K - \frac{m}{cd} \right), \quad (3.7)$$

$$T^* = \left(\frac{\beta + s}{d} - \frac{r}{d} \left(1 - \frac{N^*}{K} \right) \right) \frac{L^*}{M^*}. \quad (3.8)$$

These concentrations are given in terms of parameters and other species concentrations for ease of reading.

The next region of unique dynamics occurs when $K_0 < K < \tilde{K}$ for

$$\tilde{K} = 10^n \text{ cells/ml} \quad (3.9)$$

Here $n \approx 7 + y$ and $\chi = 10^{-y}$ for $\chi \in (0, 1]$ (see Appendix C.2.3). The value of \tilde{K} depends on the type of lysogen immunity. As the immunity becomes predominately external (χ decreases), \tilde{K} increases, and as the lysogen immunity becomes internal (χ increases), \tilde{K} approaches 10^7 cells/ml.

In this region the equilibrium coexistence concentrations given in Equations (3.5)–(3.8) can be simplified to illustrate the dynamics. These approximate concentrations are given in the first column of Table 3.2.

The expression of M^* simplifies to an expression given in terms of only phage parameters. This implies that the phage populations exhibit top down control over the sensitive bacteria population in this region. The simplified expressions for V^* and T^* demonstrate that both phage populations grow linearly with carrying capacity. In Figure 3.2 (a) the use of a value of $\chi = 0.5$ implies that $n = 7.3$ in Equation (3.9). From $K_0 < K < 10^{7.3}$ cells/ml it is observed that the sensitive bacteria population remains constant and the phage populations grow linearly, as predicted. In this region the sensitive bacteria population is much higher than the phage populations, resulting in a higher chance of a

Table 3.2. Approximate Expressions of Equations (3.5)–(3.8) for different values of K

	$K_0 < K < \tilde{K}$	$K > \tilde{K}$
M^*	$\frac{m}{cd}$	$\frac{\chi}{c} \left(1 - \frac{s}{r}\right) K$
V^*	$\frac{c(s-\beta)}{m} \left(1 - \frac{s}{r}\right) K$	$\frac{c(s-\beta)}{\chi d}$
L^*	$\left(1 - \frac{s}{r}\right) K - \frac{m}{cd}$	$\left(1 - \frac{s}{r}\right) K$
T^*	$\frac{c\beta}{m} \left(1 - \frac{s}{r}\right) K$	$\frac{c\beta}{\chi d}$

bacteria-phage encounter. Unlike what was observed in the lytic world, the phage populations are able to control the sensitive bacteria population without saturating in the system.

The final region in the system occurs when $K > \tilde{K}$, and the simplified equilibrium concentrations here are given in the second column of Table 3.2. The behavior of the sensitive bacteria and phage populations switch in this region; M^* grows linearly with K and the values of V^* and T^* remain constant. In Figure 3.2 (a) for $K > 10^{7.3}$ this predicted switch is observed. In this region the high concentrations of lysogens greatly diminishes the chance of a phage and sensitive bacteria encounters. Phages instead encounter lysogens and experience an increased negative effect from the lysogen's internal immunity. When lysogens exhibit purely external immunity ($\chi = 0$), however, the phages are able to exhibit top-down control over the sensitive bacteria and grow linearly with the carrying capacity for $K > K_0$.

The VMR of this system is given by the ratio of the total phage population (virulent and temperate) and the total bacteria population (sensitive bacteria and lysogens). Figure 3.2 (b) displays this ratio as a function of the carrying capacity of the system. When $K_0 < K < \tilde{K}$ the VMR remains constant, and then decreases for $K > \tilde{K}$. In both regions the values are on the order of 10^{-5} - 10^{-4} as a result of the extreme difference in the sizes of the bacteria and phage populations. These predicted VMRs are many magnitudes smaller than those observed in the environment [12, 20]. While this model incorporates many well understood mechanisms in bacteria-phage interactions, it does not capture the abundances of the species in a satisfactory way. The fact that the predicted phage populations are so low indicates that there may be some mechanism missing in the model. One mechanism that could be included is the lifestyle choice of the temperate phage. The next section discusses how the dynamics of the system change by incorporating this decision.

3.3 TEMPERATE PHAGES HAVE LIFESTYLE DECISION

Here temperate phages are given the ability to choose between lytic and lysogenic replication in the model. It is assumed that a fraction of the temperate phages will choose to become lysogenic, and the rest will follow a lytic lifestyle. This fraction of lysogeny is represented by the parameter f and the decision is incorporated into Equation (3.4) below:

$$\begin{aligned}
 \frac{dM}{dt} &= r \left(1 - \frac{N}{K} \right) M - dMV - dMT + sL, \\
 \frac{dV}{dt} &= cdMV - \chi dVL - mV, \\
 \frac{dL}{dt} &= r \left(1 - \frac{N}{K} \right) L - \beta L + f dMT - sL, \\
 \frac{dT}{dt} &= c\beta L - \chi dTL - \overbrace{f dMT}^{\text{lysogenic lifestyle}} + \overbrace{(1-f)cdMT}^{\text{lytic lifestyle}} - mT.
 \end{aligned} \tag{3.10}$$

The equilibrium populations of the model and the analysis of their stability is studied using standard techniques from the theory of dynamical systems and numerical stability analysis (see Appendix C.3).

The dynamics of this system for low carrying capacities is identical to those described in Section 3.2. There is a critical concentration $K_0 = \frac{m}{cd}$ that the sensitive bacteria population must reach in order for phages and lysogens to survive in the system. Once $K > \frac{m}{cd}$ the fraction of lysogeny, f , dictates how the system behaves. To illustrate this the stable concentrations of all four populations are plotted as a function of f for $K = 10^7$ cells/ml in Figure 3.3 (a). A sampling of 10^3 parameter combinations is completed for each value of f using a Latin Hypercube Sampling Scheme (Appendix E), and the median values from the sampling are plotted.

In Figure 3.3 (a) it is observed that for values of f less than approximately 0.1 only sensitive bacteria, lysogens, and temperate phages remain stably in the system. Low values of f correspond to a system in which most temperate phages choose lytic replication. This results in an increase in free temperate phages in the environment, escalating the competition between the two species of phages. Temperate phages are also added to the system when a prophage spontaneous induces a lysogen, giving them an advantage over the virulent phages. This lead to virulent phage extinction for low values of f . For $f > 0.1$ virulent phages can survive in the system and for $f > 0.2$ can reach higher concentrations than the temperate phages. As more temperate phages choose lysogenic replication the virulent and temperate phage populations move towards the values given in Equations (3.6) and (3.8), respectively. These concentrations correspond to a value of $f = 1$. Introducing this lifestyle decision of the temperate phages alters the distribution of the phage populations in the system, but has no

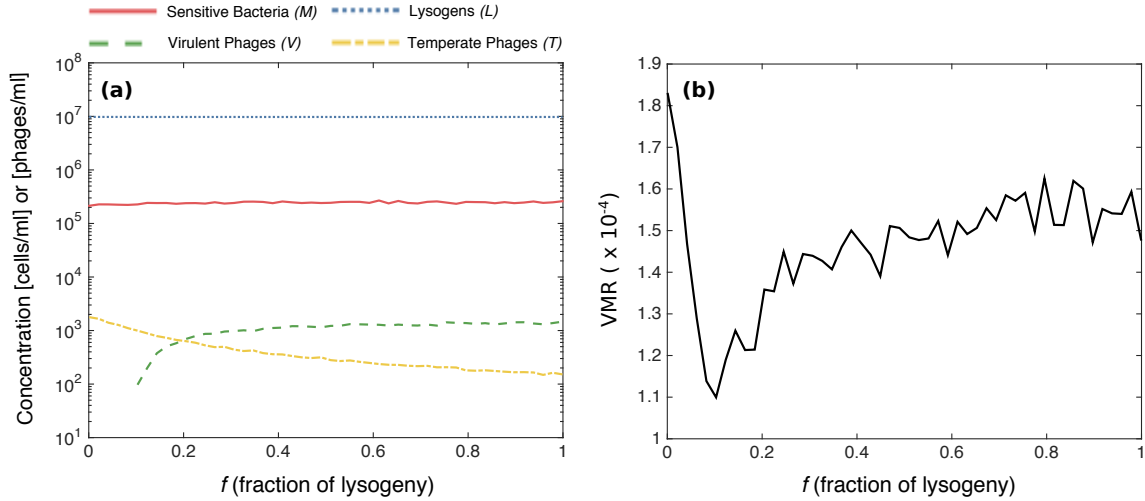


Figure 3.3. Effect of the lytic-lysogenic decision on the dynamics of a mixed model. (a) The equilibrium concentrations of sensitive bacteria (red), virulent phages (green), lysogens (blue), and temperate phages (yellow) as a function of the fraction of lysogeny, f . For each value of f , 10^3 relevant environmental parameter combinations were sampled using LHS (Appendix E). (b) Virus to microbe ratio (VMR) as a function of the fraction of lysogeny f . In (a) and (b) the median values from the sampling are shown.

effect on the sensitive bacteria or lysogen population. The VMR values given in Figure 3.3 (b) are on the order of 10^{-4} just as those observed in Figure 3.2 (b). Thus this model again predicts VMR values that are too low when compared with environmental data. Incorporating the temperate phage lifestyle decision results in another failure to accurately describe the system. Other systems were explored in which f depended on bacteria and phage concentrations in the system, but these produced similar results (data not shown). In the next section another possibly important mechanism is incorporated into the model, and the effect it has on the dynamics is studied.

3.4 VIRULENT PHAGES ABLE TO INFECT LYSOGENS

The immunity of lysogens against phage infection is most effective against phages of the same or related strain as that of the lysogen's associated prophage [35]. Here it is assumed that the virulent phages are of a different strain than the temperate phages. This allows for the infection of lysogens by virulent phages in the system. The parameter $\alpha \in [0, 1]$ is used to represent the fraction of virulent phages able to infect lysogens. This mechanism is incorporated into Equation (3.10) and the updated model is given below:

$$\begin{aligned}
\frac{dM}{dt} &= r \left(1 - \frac{N}{K} \right) M - dMV - dMT + sL, \\
\frac{dV}{dt} &= cdMV - \overbrace{(1-\alpha)\chi dVL}^{\text{immunity of } L} + \overbrace{\alpha cdVL}^{\text{infection of } L} - mV, \\
\frac{dL}{dt} &= r \left(1 - \frac{N}{K} \right) L - \beta L + fdMT - sL - \overbrace{\alpha dLV}^{L \text{ infected by } V}, \\
\frac{dT}{dt} &= c\beta L - \chi dTL - fdTM - mT + (1-f)cdTM.
\end{aligned} \tag{3.11}$$

The dynamics of this complex model are studied numerically. Simulations of Equation (3.11) indicate that introducing virulent phages that are able to infect lysogens leads to transitions in the system. Figure 3.4 (a) illustrates these transitions by plotting the equilibrium concentrations of the four populations as a function of the parameter α . The virus to microbe ratio (VMR) is also plotted as a function of α in panel (b).

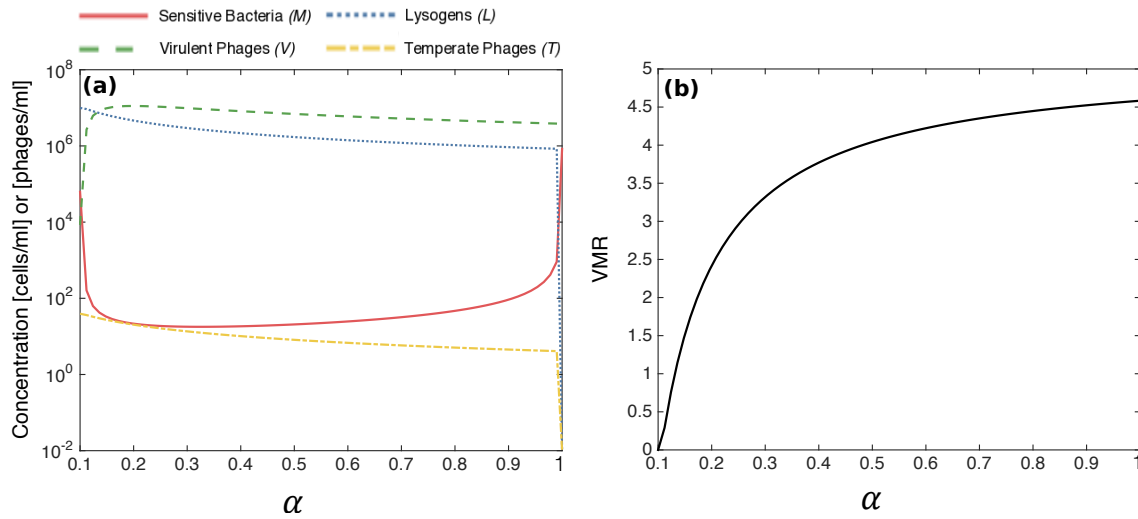


Figure 3.4. *Effect of the infection of lysogens by virulent phages on the dynamics of a mixed model.* (a) The equilibrium concentrations of sensitive bacteria (red), virulent phages (green), lysogenic bacteria (blue), and temperate phages (yellow) as a function of the fraction of virulent phages that can infect lysogens, α . (b) Virus to microbe ratio (VMR) as a function of α . Parameter values of $r = 1/24 \text{ hr}^{-1}$, $c = 20 \text{ virions}$, $d = 10^{-8} \text{ ml/cell/hr}$, $m = 1/6 \text{ hr}^{-1}$, and $K = 10^7 \text{ cells/ml}$ were used to create both plots.

The equilibrium concentrations were determined by solving the system of ordinary differential equations given in Equation (3.11) using MATLAB's ode45 solver. The system was solved over a time span long enough to allow the system to achieve equilibrium. The final concentration values were then plotted in Figure 3.4. Parameter values were taken from Table 3.1 and values of $K = 10^7 \text{ cells/ml}$ and $f = 0.5$ were used for the simulations.

For values of $\alpha < 0.1$ the fraction of virulent phages that can infect lysogens is too low to have an effect on the system and it behaves similarly to Equation (3.10). In Figure 3.4 (a) there is a sudden, drastic change in the equilibrium values at $\alpha \approx 0.12$, indicating a bifurcation has occurred. The virulent phage concentration increases and exceeds the lysogen concentration, while the sensitive bacteria concentration decreases to values many magnitudes lower. This behavior indicates that there is some threshold value α_0 that represents a transition to virulent phage dominance in the system. Here a large enough portion of the virulent phages are able to infect lysogens, resulting in an increase in the concentration of free phages. The chance of a virulent phage and sensitive bacteria encounter is then much higher and the bacteria concentration is reduced. The lysogens remain at relatively large concentrations in the system because they are still immune to infection by a portion of the virulent phages.

As α increases there is a slight reduction in the virulent phage concentration as a result of the reduction of their prey. This allows the sensitive bacteria population to increase as the value of α increases. When $\alpha = 1$ another drastic change takes place in the system as observed in Figure 3.4 (a), implying the existence of another bifurcation. At this value all virulent phages have the ability to infect lysogens and exhibit the same control over both the sensitive bacteria and lysogen populations. This initiates a competition between these two populations. However, the lysogens are at a disadvantage because of the spontaneous induction of the prophage and the effect of lysogen curing. The rates of these two mechanisms are extremely slow, but they will eventually lead to lysogen and temperate phage extinction. The only surviving populations at equilibrium are the sensitive bacteria and virulent phages, reducing the dynamics of the system to those of the lytic world (2.1).

Including the ability of a portion of the virulent phage population to infect lysogens changes the dynamics of the system from what was observed in Sections 3.2 and 3.3. The higher equilibrium concentrations of virulent phages predicted by this model gives VMR values that align with the environment [12, 20]. The parameter α also initiates transitions in the system at a larger scale than observed in the previously studied models. It would be premature, however, to conclude that Equation (3.11) exactly captures environmentally observed dynamics. In Figure 3.4 (a) the equilibrium concentrations of sensitive bacteria and temperate phages remain at extremely small values for much of the range of α . More conclusive information about the composition of systems must be analyzed in order to validate that this may be realistic in environmental systems.

The results from the analysis of this model indicate the importance of an aspect that is missing from all models studied thus far. It could be assumed that the virulent phages in this system that are able to infect lysogens gained this ability through evolution. This would result in a new species of virulent phages that would then be less effective at infecting sensitive

bacteria. This leads to specialization of the phages [5, 8]. Lysogens may then evolve to prevent this infection, necessitating another phage evolution, and the dynamics would repeat [30]. This process would result in a system of different phage species, each with a specific host species. A community model would be necessary to capture the dynamics of this system, which was already stated as a possible improvement to the models. Community models of the bacteria-phage system and their predicted dynamics are the topic of Chapter 4.

CHAPTER 4

COMMUNITY WORLDS

The results from the previous chapter indicate that a different approach must be taken in the modeling process. In the environment, bacteria and phage populations are made up of many different species. The effect of these communities may alter the predictions that were made based on the simplified single species models. To explore this effect the lytic and lysogenic worlds are extended to their respective community models. The results from the analysis of these models are used to combine the two worlds and interpret the data from [12].

4.1 LYTIC WORLD: COMMUNITY MODEL

A system consisting of n species of sensitive bacteria and n species of virulent phages is modeled. The interactions between bacteria and phage species are assumed to be one-to-one. Species of bacteria are differentiated according to the species of phages that infect them, i.e., if two bacteria are infected by the same phage species, then they belong to the same *ecological* species. The dynamics of this system are described by a system of $2n$ ordinary differential equations. Assuming that all species are homogeneously mixed, the mathematical model of the lytic world community is given below:

$$\begin{aligned} \frac{dM_i}{dt} &= \overbrace{r \left(1 - \frac{M}{K}\right) M_i}^{\text{logistic growth}} - \overbrace{dM_i V_i}^{\text{infection}}, \\ \frac{dV_i}{dt} &= \overbrace{cdM_i V_i}^{\text{lysis}} - \overbrace{mV_i}^{\text{decay}}. \end{aligned} \tag{4.1}$$

where $i = 1, 2, \dots, n$. In this model, the concentration of sensitive bacteria species i is represented by M_i , and the concentration of virulent phage species i is represented by V_i . The concentration of the bacteria community is represented by $M = \sum_{i=1}^n M_i$ and the concentration of the phage community is represented by $V = \sum_{i=1}^n V_i$. Bacteria and phage parameters are assumed to be identical across all species, and the carrying capacity, K , is assumed to correspond to the community of bacteria. The interactions between bacteria and phages in species i are identical to those described in Section 2.1. All parameters are greater than zero and typical environmental values are given in Table 4.1.

Table 4.1. Meaning of Parameters Included in the Lytic World Community Model (Equation (4.1))

Parameter	Description	Value	Reference
r	intrinsic growth rate of bacteria species	$1/24 \text{ hr}^{-1}$	[34]
K	carrying capacity of bacteria community	$10^3\text{-}10^9 \text{ cells/ml}$	
d	infection rate of virulent phage species	$10^{-8} \text{ ml/cells/hr}$	[34]
c	burst size of virulent phage species	20 virons	[34]
m	decay rate of virulent phage species	$1/6 \text{ hr}^{-1}$	[34]
n	number of species in the community		

The equilibrium populations of the model and the analysis of their stability is studied using standard techniques from the theory of dynamical systems and numerical simulations (see Appendix D.1).

In this system, different species of phages do not interact directly, and the interaction of different bacteria species only occurs through their shared energy resources, i.e., carrying capacity. This results in a system with similar dynamics to that of the single species lytic world. The threshold carrying capacity required for coexistence between all bacteria and phage species is given by $K_0 = \frac{mn}{cd}$. For $K < K_0$ the phage community cannot survive in the system, which allows the bacteria community to grow to its carrying capacity. The distribution of the bacteria species is determined by the initial species distribution (see Appendix D.1.1). This implies that the fraction of a bacteria species remains constant in the system at all times, i.e., for $t \in [0, \infty)$ the following is true:

$$\frac{M_i(t)}{M(t)} = \frac{M_{i0}}{M_0},$$

where M_{i0} is the initial concentration for bacteria species i , and M_0 is the initial total concentration of bacteria.

When $K > K_0$ there is coexistence between all bacteria and phage species for certain value of n . The equilibrium concentrations at coexistence are identical across all species and are given in terms of parameters below:

$$M_i^* = \frac{m}{cd}, \quad (4.2)$$

$$V_i^* = \frac{r}{d} \left(1 - \frac{mn}{cdK} \right). \quad (4.3)$$

These expressions are identical to those of bacteria and phages in the lytic world at coexistence. It can thus be seen that each species of phages exhibits top-down control over the corresponding bacteria species. Using Equations (4.2) and (4.3), the concentrations of the

bacteria and phage communities at coexistence are given by the following:

$$M^* = \frac{mn}{cd}, \quad (4.4)$$

$$V^* = \frac{rn}{d} \left(1 - \frac{mn}{cdK}\right) = \frac{rc}{m} M^* \left(1 - \frac{M^*}{K}\right). \quad (4.5)$$

Equations (4.4) and (4.5) depend on the number of species in the system, n . In order to illustrate this dependence, the populations of the bacteria and phage communities are plotted as a function of n in Figure 4.1 (a). This plot was created using the baseline parameter values given Table 4.1 and a value of $K = 10^7$ cells/ml.

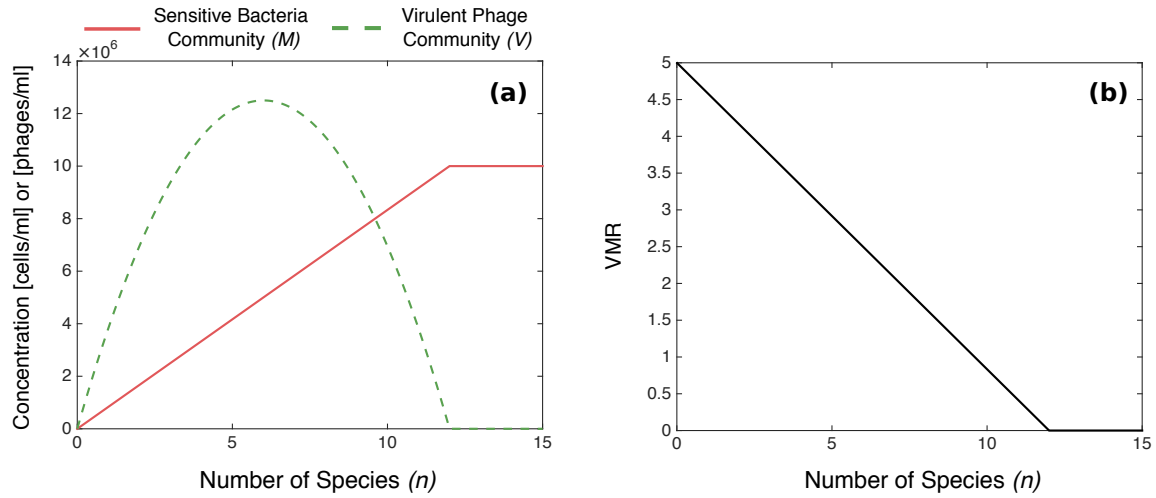


Figure 4.1. Impact of the number of species in the lytic world community. (a) The equilibrium concentrations of the sensitive bacteria community (red), and the virulent phage community (green) as a function of the number of species, n . (b) The virus to microbe ratio (VMR) as a function of n . Parameter values of $r = 1/24 \text{ hr}^{-1}$, $c = 20$ virions, $d = 10^{-8} \text{ ml/cell/hr}$, $m = 1/6 \text{ hr}^{-1}$, and $K = 10^7$ cells/ml were used in panels (a) and (b).

From Equation (4.4) it is observed that the bacteria community grows linearly with n . More species equates to more bacteria in the community. However, this growth cannot continue indefinitely because the value of M^* is limited by the carrying capacity of the system. For $n \geq \frac{cdK}{m}$, the population of the bacteria community ceases growth and remains at K . For the parameter values used in Figure 4.1 (a) this transition occurs at $n = 12$, which explains the change in the behavior of M^* at this value. In the lytic world, the sensitive bacteria were unable to utilize all of the energy resources in the system because of the top-down control by the phages. In the lytic community model the sensitive bacteria community can overcome this limitation by the introduction of more species into the system.

As seen in Equation (4.5), the expression for the phage community is given by a downward facing parabola in n . The parabola attains positive values between its roots at

$n = 0$ and $n = \frac{cdK}{m}$, implying that the phage community only survives in this range. These n values correspond to the values for which M^* has linear growth. Figure 4.1 (a) displays the phage community's parabolic relationship with n . As the number of species in the system increases, the phage community population also increases until $n = \frac{cdK}{2m}$. This value represents the optimal number of species for the phage community. Here, the phage community, V , is at a maximum size, given by the following:

$$V_{max} = \frac{rc}{4m} K. \quad (4.6)$$

For the parameter values used in Figure 4.1 (a) the above mentioned expressions predict that the phage community will attain a maximum value of 12.5×10^6 phages/ml in a community with 6 species. When the number of species in the community exceeds this optimal value, the population of the phage community will begin to decrease in size. Each species of phage must encounter its corresponding species of bacteria in order to reproduce and overcome its decay rate. Thus, as more species are added to the system, the chance that a phage encounters the correct species of bacteria decreases. This can be seen from virus to microbe ratio for each species, VMR_i , which is given by the following:

$$VMR_i = \frac{V_i^*}{M_i^*} = \frac{rc}{m} \left(1 - \frac{mn}{cdK} \right). \quad (4.7)$$

This expression has a negative linear relationship with the number of species in the system. As n increases, the relative number of phage from species i with respect to its corresponding bacteria species decreases. The population of the phage community will continue to decrease until it becomes extinct when $n = \frac{cdK}{m}$. In Figure 4.1 (a) this extinction occurs at $n = 12$.

The VMR for the community is given in terms of parameters by the following expression:

$$VMR = \frac{V^*}{M^*} = \frac{rc}{m} \left(1 - \frac{mn}{cdK} \right). \quad (4.8)$$

This expression behaves identically to Equation (4.7), which is shown for specific parameter values in Figure 4.1 (b).

In order to better understand the prevalence of phage community extinction in the environment, a sampling approach is used. Different parameter samples are created using a Latin Hypercube Sampling Scheme (Appendix E) for different values of n . For each sample it is determined if a phage community with those parameter values would survive. The fraction of surviving phage communities out of the total samples is calculated and plotted as a function of n in Figure 4.2. Systems with $K = 10^6, 10^7$ and 10^8 cells/ml are compared. The sampling indicates that there is a limited range of n values for which nearly all the communities can survive. Increasing K makes this range larger, but systems with larger carrying capacities will still experience the effect of phage extinction.

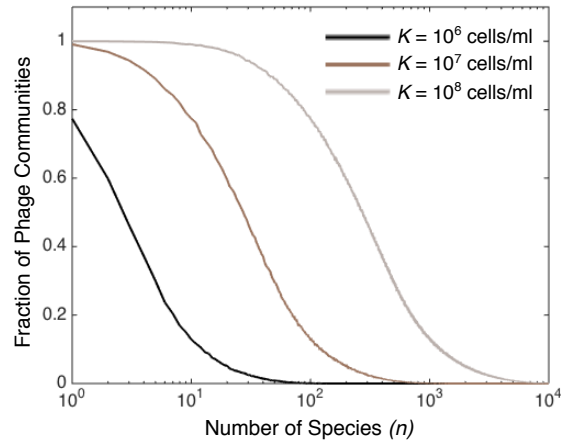


Figure 4.2. Impact of the number of species on the fraction of surviving phage communities. For each value of n the populations of 10^4 communities with different parameters are calculated. The number of surviving phage communities out of the total is plotted for $K = 10^6$ cells/ml (black), $K = 10^7$ cells/ml (brown) and $K = 10^8$ cells/ml (grey).

The analysis of the lytic community model reveals that there is a point, determined by the number of species, n , where choosing a lytic lifestyle is no longer advantageous to the phage community. At this point it may be necessary to transition to a lysogenic lifestyle. A discussion of the lysogenic world community is given in the next section.

4.2 LYSOGENIC WORLD: COMMUNITY MODEL

A system consisting of n species of lysogens and n species of temperate phages is modeled. The interactions between lysogen and phage species are assumed to be one-to-one. Species of lysogens are differentiated according to the species of the prophage that resides inside of them, i.e., if two lysogens contain the same species of prophage, then they belong to the same species. The dynamics of this system are described by a system of $2n$ ordinary differential equations. Assuming all species are homogeneously mixed, the mathematical model of the lysogenic community world is given below:

$$\begin{aligned}
\frac{dL_i}{dt} &= \overbrace{r \left(1 - \frac{L}{K}\right)}^{\text{logistic growth}} L_i - \overbrace{\beta L_i}^{\text{induction}}, \\
\frac{dT_i}{dt} &= \overbrace{c\beta L_i}^{\text{lysis}} - \overbrace{mT_i}^{\text{decay}} - \overbrace{\chi dT_i L_i}^{\text{immunity of } L_i}.
\end{aligned} \tag{4.9}$$

where $i = 1, 2, \dots, n$. In this model the concentration of lysogen species i is represented by L_i and the concentration of temperate phage species i is represented by T_i . The concentration of the lysogen community is represented by $L = \sum_{i=1}^n L_i$ and the concentration of the phage community is represented by $T = \sum_{i=1}^n T_i$. It is assumed that lysogen and phage parameters are identical across all species, and that the carrying capacity, K , corresponds to the community of lysogens. The interactions between lysogens and phages from species i are identical to those described in Section 2.2. All parameters excluding χ are always greater than zero and typical values are given in Table 4.2.

Table 4.2. Meaning of Parameters Included in the Lysogenic Community World Model (Equation (4.9))

Parameter	Description	Value	Reference
r	intrinsic growth rate of lysogen species	$1/24 \text{ hr}^{-1}$	[34]
K	carrying capacity of lysogen community	$10^3\text{-}10^9 \text{ cells/ml}$	
β	induction rate of prophage species	$(1/24) \times 10^{-6} \text{ hr}^{-1}$	[22, 23]
c	burst size of temperate phage species	20 virions	[34]
m	decay rate of temperate phage species	$1/6 \text{ hr}^{-1}$	[34]
d	infection rate of temperate phage species	$10^{-8} \text{ ml/cells/hr}$	[34]
χ	lysogen species immunity	$[0, 1]$	
n	number of species in the community		

The equilibrium populations of the model and the analysis of their stability is studied using standard techniques from the theory of dynamical systems and numerical simulations (see Appendix D.2)

There is always coexistence between all lysogen and temperate phage species in this system. The population of the lysogen community can be expressed in terms of parameters by the following expression:

$$L^* = \left(1 - \frac{\beta}{r}\right) K. \tag{4.10}$$

This is the same equilibrium concentration of the lysogens that was found the single species model, but here it represents the population of the community. The distribution of lysogen species in this system is determined by the initial distribution of species (see Appendix D.2.1).

Let L_{i0} represent the initial concentration of species i and let L_0 represent the initial concentration of the community. The initial fraction of lysogen species i in the system is given by $f_i = \frac{L_{i0}}{L_0}$ and is constant for all time. The populations of each lysogen species at equilibrium can be expressed by the following:

$$L_i^* = f_i L^* = f_i \left(1 - \frac{\beta}{r}\right) K. \quad (4.11)$$

Using Equation (4.11) the population of each temperate phage species can be expressed in terms of parameters by the following expression:

$$T_i^* = \frac{c\beta L_i^*}{m + \chi d L_i^*} = \frac{c\beta f_i \left(1 - \frac{\beta}{r}\right) K}{m + \chi d f_i \left(1 - \frac{\beta}{r}\right) K}. \quad (4.12)$$

The population of the temperate phage community will therefore depend on the distribution of the lysogen species. For example, if the lysogen species were equidistributed, that is, $f_i = \frac{1}{n}$ for all i , then $T_i^* = \frac{c\beta \left(1 - \frac{\beta}{r}\right) \frac{K}{n}}{m + \chi d \left(1 - \frac{\beta}{r}\right) \frac{K}{n}}$. The population of the temperate phage community would then be expressed by $T^* = \frac{c\beta L^*}{m + \chi d \frac{L^*}{n}}$.

In this community model the population of the lysogen community behaves identically to that of the lysogen population in the single species model. The value of L^* grows linearly with the carrying capacity and the lysogen community is able to utilize almost all of the available energy resources. The number of species in the community has no effect on the size or behavior of L^* . It is difficult to make a general statement about the effect of n on the population of the temperate phage community. However, based on the behavior of the lysogen community, it is predicted that altering the number of species would have minimal effect on T^* . As discussed in Section 2.2, the temperate phage community is at an advantage in this system because the number of prophages grows linearly with K . The similar behavior of the single species and community models motivates a combination of the lytic and lysogenic community worlds discussed in the next section.

4.3 COMBINING THE LYTIC AND LYSOGENIC COMMUNITY WORLDS

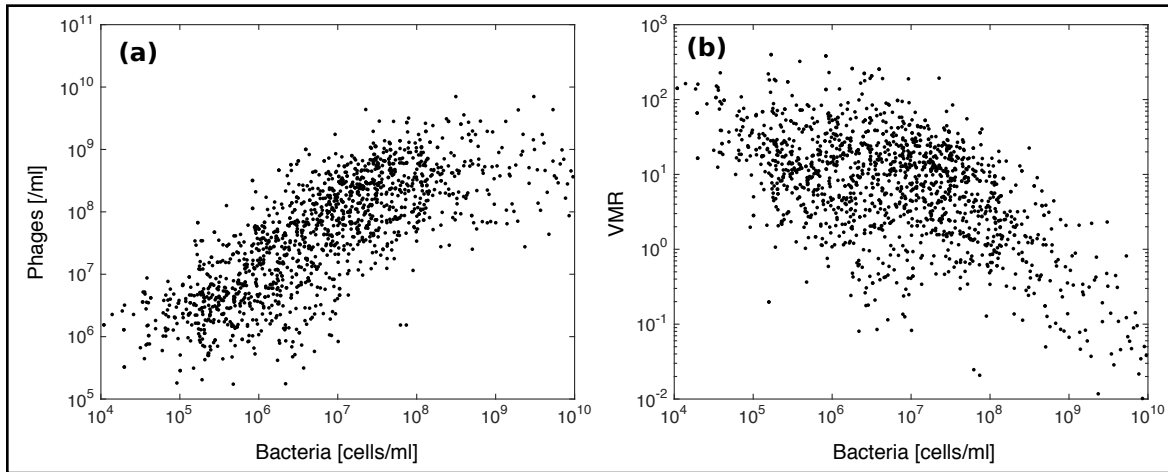
The dynamics of the lytic and lysogenic community worlds indicate that a combination of these models may successfully recover the trends of the environmental data, as shown below [12]. In Section 2.3 the combination of the single species lytic and lysogenic worlds predicted much lower VMRs than the data indicated. In the lytic community world, increasing the number of species results in larger bacteria concentrations. This allows for larger concentrations of phages for certain numbers of species in the community. Thus combining the community models provides a mechanism to address the shortcoming of the single species model.

A specific combination of the lytic and lysogenic community worlds is studied as an example of what these models would predict. The data is assumed to come from bacteria-phage systems with varying numbers of communities. Here, four systems with 1, 10, 50, and 100 species of bacteria and phage are simulated. In some cases the bacteria communities are not able to utilize all the energy resources in the system because of the top down control of the phages. A similar approach to that discussed in Section 2.3 is taken to combine the community models. Lysogen communities can use a fraction of the remaining resources in the system. This fraction depends on the total resources of the system and increases for higher concentrations of bacteria [10, 18]. The total bacteria population is then made up of sensitive bacteria and lysogens, and the total phage population is made up of virulent and temperate phages. A Latin Hypercube Sampling Scheme (Appendix E) is used to create parameter samples that simulate the variability in these systems. The samples are then used to determine the bacteria and phage community populations. The results of this combination as well as the environmental data from [12] are displayed in Figure 4.3. The total phage community concentrations are plotted as a function of the total bacteria community concentrations in panel (a). Similar trends are observed to those in the environmental data in panel (c). In both plots the phage concentration grows approximately linearly for bacteria concentrations in the range 10^4 - 10^8 cells/ml. For bacteria concentrations larger than 10^8 cells/ml, the phage concentrations appear to saturate at the range 10^8 - 10^{10} phages/ml in (a) and (c). In Figure 4.3 (b) the VMRs of the sampling are plotted as a function of bacteria concentration, which can be compared to the environmental VMRs in panel (d). In both plots the VMRs are in the range 1-100 for lower bacteria concentrations and then decrease from 1 to 10^{-2} for higher concentrations. The ranges predicted by the models are in qualitative agreement with the environmental data. There is a difference in the grouping of the data points between the two plots. While the environmental data is concentrated at lower bacteria concentrations, the model data is more evenly distributed across all concentrations. The distribution of the environmental data is most likely due to the oversampling of marine ecosystems [12, 13].

4.4 A PROPOSED SPECIATION MODEL

The results presented in Section 4.3 lead to the proposal of a speciation model to explain the dynamics of the system. As discussed in Section 2.1, the phage population will saturate in a single species system that is dominated by phages choosing lytic replication. The presence of excess energy resources in the system then encourages the emergence of lysogens that are able to utilize these resources. A portion of the phage population then evolves in order to overcome the immunity of the lysogens. This evolution specializes the phages to be most effective at infecting lysogens [5, 8]. Thus, a new pair of bacteria-phage species is introduced

Community World



Environmental Data

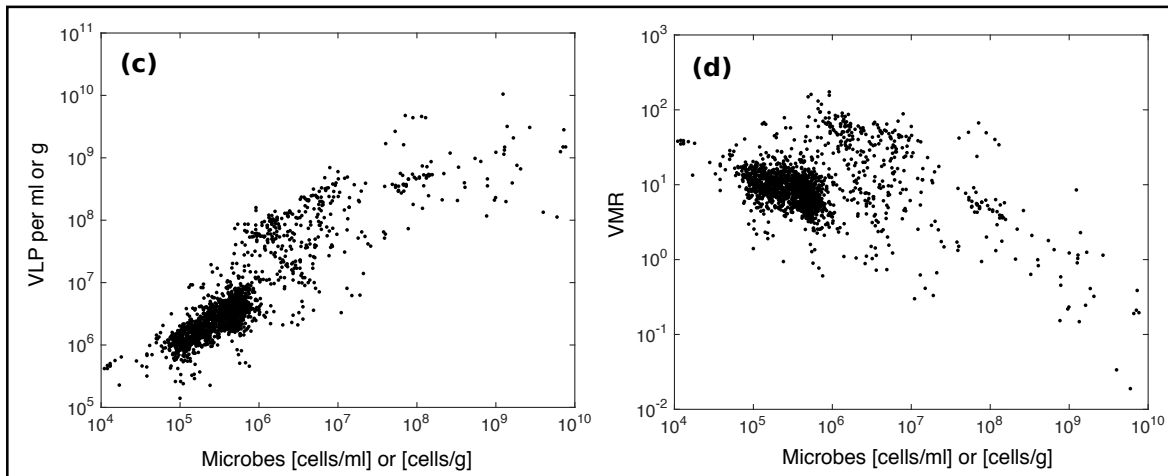


Figure 4.3. Predicted bacteria and phage concentrations from the combination of the lytic and lysogenic community worlds compared to environmental data. (a) Phage concentration as a function of bacteria concentration from the combination. (b) Virus to microbe ratio (VMR) as a function of bacteria concentration from the combination. Data was generated using 2000 relevant environmental parameter combinations created from LHS (Appendix E) and a combination scheme described in Section 4.3. (c) Concentration of virus-like particles (VLPs) as a function of microbe concentration from environmental data. (d) Virus to microbe ratio (VMR) as a function of bacteria concentration from environmental data. Data source: B. Knowles et al., *Lytic to temperate switching of viral communities*, Nature, 531 (2016), pp. 466–470.

into the system, according to the classification of species based on predation. The addition of resources and the evolution of bacteria to acquire new immunity would cause the process of speciation to repeat. It is proposed that these dynamics can be observed in Figure 4.3 (c) for bacteria concentrations in the range 10^4 - 10^8 cells/ml. Here the population of the phage

community increases as a result of the addition of new species into the system. As discussed in Section 4.1, there is an optimal number of species for which a lytic phage community reaches a maximum value. Exceeding this number leads to the decline and eventual extinction of the phage community. Thus, it would be detrimental to the phages to continue the process of speciation indefinitely. It is predicted that the phages would switch to lysogenic replication here in order to remain in the system. The immunity of the lysogens allows the phage community to increase in the system as prophages, rather than free phages. This cessation of the process of speciation is proposed to correspond to the leveling off of phage concentrations for bacteria concentrations from 10^8 - 10^{10} cells/ml in Figure 4.3 (c).

This speciation model predicts that in bacteria-phage systems, lysogeny encourages the evolution of new species. This prediction could be tested through experiments that determine the prophage abundance in communities of bacteria. The presence of prophages, either active or inactive, in a bacterium's genome can indicate that the bacteria has evolved multiple times through the mechanism propose here [30]. Systems with varying bacteria concentrations could be compared. Communities from systems with low concentrations of bacteria would be expected to have few prophages present in their genomes. This would imply that few evolutions of new species have occurred in ecosystems. If the model is valid, the abundance of prophages would then increase as the concentration of bacteria increased. This trend would indicate that speciation as a result of lysogeny can push a community to higher bacteria concentrations. The results from such experiments would provide valuable insight to both the biologists that study these systems and the mathematicians that model them.

CHAPTER 5

CONCLUSIONS AND FUTURE WORK

In this thesis, different mathematical models were analyzed in order to capture the transition in phage populations from lytic to lysogenic replication as bacterial abundance increases. A lytic model shows that this type of replication limits the concentrations that phages can reach in the system. A lysogenic model indicates that lysogens, and therefore prophages, are able to flourish in systems with large amounts of energy resources. A compartmental model that combines the lytic and lysogenic models illustrates similar dynamics to those seen in the environmental data from [12]. However, the model predicts phage concentrations that are magnitudes lower than those given in the data.

Mixing the lytic and lysogenic models to include the interactions of sensitive bacteria, virulent phages, lysogens, and temperate phages also predicts unrealistic values for the system. Lysogens are assumed to have immunity from infection by phages, which allows bacteria to dominate the system. The model therefore predicts virus to microbe ratios that are many orders of magnitude lower than environmental observations. Including the assumption that a portion of the virulent phages can infect the lysogens in the mixed model elicits transitions in the system. This indicates a potential underlying process of speciation that can be modeled by a bacteria-phage community.

A lytic community model predicts that introducing more species to the system increases both the bacteria and phage populations. There is also an optimal number of species that allows the phage community to reach a maximum concentration. However, exceeding this number results in a decrease of the phage population until it eventually becomes extinct. The lysogen community model has overall dynamics that are identical to the single species model. A compartmental model of the lytic and lysogenic communities is successful in reproducing the observational data [12].

The success of the compartmental community model leads to the proposal of a speciation model to explain the transition from lytic to lysogenic replication in phage populations. The presence of excess energy resources in a lytic community encourages the emergence of lysogens. Phages evolve to gain the ability to infect the previously immune lysogens. A new pair of predator-prey species, given by the evolved phages and lysogens, has then been added to the system. The process of speciation continues until it becomes disadvantageous to the phage population, as it will lead to their extinction. Phages transition

to lysogenic replication here in order to remain in the system as prophages that are protected by the lysogens.

There are many ways to expand upon the work completed in this thesis. In the environment, bacteria populations are also effected by grazers that feed on them [28]. The effect of grazing could be incorporated into all models and compared to the results discussed in this thesis. The parameter values were assumed to be the same across populations in many of the models. This was done to simplify the analysis of the models, but the populations could also be differentiated by their parameters. Each model studied in this thesis is composed of ordinary differential equations that only depend on time, not space. This requires the assumption that all populations are homogeneously mixed in the system. The effect of the spatial distribution of populations in the system could be explored by extending each ordinary differential equation to its respective partial differential equation. Preliminary results indicate that such models may reduce the time for the system to reach equilibrium. Finally, a community mixed model could be studied as a way to build off the positive results of the lytic and lysogenic community compartmental model. This model would include species of sensitive bacteria, virulent phages, lysogens, and temperate phages, and describe the interactions across all species. Such a model would illustrate a more formal way to model the transition in phage populations from lytic to lysogenic replication in the system.

The results discussed in this thesis will hopefully assist biologists studying bacteria-phage systems to design experiments and analyze acquired data. This may lead to a more complete understanding of these complex systems.

BIBLIOGRAPHY

- [1] O. BERGH, K. Y. BORSHEIM, G. BRATBAK, AND M. HELDAL, *High abundance of viruses found in aquatic environments*, Nature, 340 (1989), pp. 467–468.
- [2] L. BOSSI ET AL., *Prophage contribution to bacteria; population dynamics*, Journal of Bacteriology, 185 (2003), pp. 6467–71.
- [3] G. BRATBAK, M. HELDAL, S. NORLAND, AND T. F. THINGSTAD, *Viruses as partners in spring bloom microbial trophodynamics*, Applied and Environmental Microbiology, 56 (1990), pp. 1400–1405.
- [4] H. BRUSSOW, C. CANCHAYA, AND W. HARDT, *Phages and the evolution of bacterial pathogens: from genomic rearrangements to lysogenic conversion*, Microbiology and Molecular Biology Reviews, 68 (2004), pp. 560–602.
- [5] A. BUCKLING AND P. B. RAINEY, *Antagonistic coevolution between a bacterium and a bacteriophage*, Proceeding of the Royal Society B: Biological Sciences, 269 (2002), pp. 931–936.
- [6] A. CAMPBELL, *General aspects of lysogeny*, in The Bacteriophages, R. Calendar, ed., Oxford University Press, Inc., New York, New York, second ed., 2006, ch. 7, pp. 66–73.
- [7] M. DE PAEPE AND F. TADDEI, *Viruses' life history: Towards a mechanistic basis of a trade-off between survival and reproduction among phages*, PLOS Biology, 4 (2006), pp. 1248–1256.
- [8] S. DUFFY AND P. E. TURNER, *Phage evolutionary biology*, in Bacteriophage Ecology: Population Growth, Evolution, and Impact of Bacterial Viruses (Advances in Molecular and Cellular Microbiology), S. T. Abedon, ed., Cambridge University Press, United Kingdom, first ed., 2008, ch. 6, pp. 147–176.
- [9] L. R. E. AND B. R. LEVIN, *Constraints on the coevolution of bacteria and virulent phage: A model, some experiments, and predictions for natural communities*, American Naturalist, 125 (1985), pp. 585–602.
- [10] A. F. HAAS ET AL., *Global microbialization of coral reefs*, Nature Microbiology, (2016).
- [11] A. JAFFE-BRACHET AND S. BRIAUX-GERBAUD, *Curing of pI prophage from Escherichia coli k-12 recA(pI) lysogens superinfected with pI bacteriophage*, Journal of Virology, 37 (1981), pp. 854–859.
- [12] B. KNOWLES ET AL., *Lytic to temperate switching of viral communities*, Nature, 531 (2016), pp. 466–470.
- [13] B. KNOWLES ET AL., *Variability and host density independence in inductions-based estimates of environmental lysogeny*, Nature Microbiology, 2 (2017).

- [14] P. L. M. AND J. A. FUHRMAN, *Viral mortality of marine bacteria and cyanobacteria*, Current Opinion in Microbiology, 38 (2017), pp. 66–73.
- [15] M. D. MCKAY, R. J. BECKMAN, AND W. J. CONOVER, *A comparison of three methods for selecting values of input variables in the analysis of output from a computer code*, Technometrics, 21 (1979), pp. 239–245.
- [16] R. V. MILLER AND M. J. DAY, *Contribution of lysogeny, pseudolysogeny, and starvation to phage ecology*, in Bacteriophage Ecology: Population Growth, Evolution, and Impact of Bacterial Viruses (Advances in Molecular and Cellular Microbiology), S. T. Abedon, ed., Cambridge University Press, United Kingdom, first ed., 2008, ch. 5, pp. 114–143.
- [17] J. D. MURRAY, *Mathematical Biology: I. An Introduction*, Springer-Verlag, New York, NY, third ed., 2002.
- [18] C. E. NELSON ET AL., *Coral and macroalgal exudates vary in neutral sugar composition and differently enrich reef bacterioplankton lineages*, The ISME Journal, 7 (2013), pp. 962–979.
- [19] J. NOCEDAL AND S. J. WRIGHT, *Numerical Optimization*, Springer, New York, NY, second ed., 2006.
- [20] K. J. PARIKKA, M. LE ROMANCER, N. WAUTERS, AND S. JACQUET, *Deciphering the virus-to-prokaryote ratio (vpr): Insights into virus-host relationships in a variety of ecosystems*, Biological Reviews, 92 (2017), pp. 1081–1100.
- [21] J. H. PAUL AND M. WEINBAUER, *Detection of lysogeny in marine environments*, Manual of Aquatic Viral Ecology, 4 (2010), pp. 30–33.
- [22] A. ROKNEY ET AL., *Host responses influence on the induction of lambda prophage*, Molecular Microbiology, 68 (2008), pp. 29–36.
- [23] J. L. ROSNER, *Formation, induction, and curing of bacteriophage ϕ 1 lysogens*, Virology, 48 (1972), pp. 679–689.
- [24] G. P. C. SALMOND AND P. C. FINERAN, *A century of the phage: Past, present, and future*, Nature Reviews Microbiology, 13 (2015), pp. 777–786.
- [25] F. M. STEWART AND B. R. LEVIN, *The population of bacterial viruses: Why be temperate*, Theoretical Population Biology, 26 (1984), pp. 93–117.
- [26] S. H. STROGATZ, *Nonlinear Dynamics and Chaos: With Applications to Physics, Biology, Chemistry, and Engineering*, Westview Press, Boulder, CO, second ed., 2015.
- [27] W. C. SUMMERS, *Phage and the early development of molecular biology*, in The Bacteriophages, R. Calendar, ed., Oxford University Press, Inc., New York, New York, second ed., 2006, ch. 1, pp. 3–7.
- [28] T. THINGSTAD, G. BRATBAK, AND M. HELDAL, *Aquatic phage ecology*, in Bacteriophage Ecology: Population Growth, Evolution, and Impact of Bacterial Viruses (Advances in Molecular and Cellular Microbiology), S. T. Abedon, ed., Cambridge University Press, United Kingdom, first ed., 2008, ch. 10, pp. 251–280.

- [29] T. F. THINGSTAD, *Elements of a theory for the mechanisms controlling abundance, diversity, and biogeochemical role of lytic bacterial viruses in aquatic systems*, Limnology and Oceanography, 45 (2000), pp. 1320–1328.
- [30] M. TOUCHON, J. A. MOURA DE SOUSA, AND E. P. C. ROCHA, *Embracing the enemy: The diversification of microbial gene repertoires by phage-mediated horizontal gene transfer*, Applied and Environmental Microbiology, 56 (1990), pp. 1400–1405.
- [31] R. L. VEGA THURBER, J. P. PAYET, A. R. THURBER, AND A. M. S. CORREA, *Virus-host interactions and their roles in coral reef health and disease*, Nature Reviews Microbiology, (2017).
- [32] Z. WANG AND N. GOLDENFIELD, *Fixed points and limit cycles in the population dynamics of lysogenic viruses and their hosts*, Physical Review E, 82 (2010).
- [33] M. G. WEINBAUER, *Ecology of prokaryotic viruses*, FEMS Microbiology Reviews, 28 (2004), pp. 127–181.
- [34] J. WEITZ, S. J. BECKETT, J. R. BRUM, B. B. CAEL, AND J. DUSHOFF, *Lysis, lysogeny, and virus-microbe ratios*, bioRxiv, (2016).
- [35] J. S. WEITZ, *Quantitative Viral Ecology: Dynamics of Viruses and Their Microbial Hosts*, Princeton University Press, Princeton, New Jersey, 2015.
- [36] J. S. WEITZ AND J. DUSHOFF, *Alternative stable states in host-phage dynamics*, Theoretical Ecology, 1 (2008).
- [37] J. S. WEITZ ET AL., *A multitrophic model to quantify the effects of marine viruses on microbial food webs and ecosystem processes*, The ISME Journal, (2014).
- [38] B. A. WIGGINS AND M. ALEXANDER, *Minimum bacterial density for bacteriophage replication: Implications for significance of bacteriophages in natural ecosystems*, Applied and Environmental Microbiology, 49 (1985), pp. 19–23.
- [39] S. WIGGINS, *Introduction to Applied Nonlinear Dynamical Systems and Chaos*, Springer-Verlag, New York, NY, second ed., 2003.
- [40] K. E. WOMMACK AND R. R. COLWELL, *Virioplankton: Viruses in aquatic ecosystems*, Microbiology and Molecular Biology Reviews, 64 (2000), pp. 69–114.

APPENDIX A
BACKGROUND MATHEMATICS

BACKGROUND MATHEMATICS

Much of the analysis completed in this thesis relates to the study of nonlinear dynamical systems. The theory that is necessary to understand the mathematics used throughout this work is given here.

A.1 DYNAMICAL SYSTEMS

Dynamical systems describe how a system changes in time. The dynamical systems studied in this thesis are given by systems of autonomous, nonlinear ordinary differential equations. Such a system can be represented by the following equation:

$$\frac{d\mathbf{x}}{dt} = \mathbf{f}(\mathbf{x}) \tag{A.1}$$

where $\mathbf{x} \in \mathbb{R}^n$ and $\mathbf{f}(\mathbf{x}) = (f_1(\mathbf{x}), \dots, f_n(\mathbf{x}))$. Solutions of Equation (A.1) are given by trajectories that move through an n -dimensional phase space. The following theorem can be used to guarantee that Equation (A.1) has a unique solution.

Theorem A.1. (Existence and Uniqueness) *Consider the initial value problem Equation (A.1), $\mathbf{x}(0) = \mathbf{x}_0$. Suppose that \mathbf{f} is continuous and that all its partial derivatives $\partial f_i / \partial x_j$, $i, j = 1, \dots, n$, are continuous for \mathbf{x} in some open set $D \subset \mathbb{R}^n$. Then for $\mathbf{x}_0 \in D$, the initial value problem has a solution $\mathbf{x}(t)$ on some time interval $(-\tau, \tau)$ about $t = 0$, and the solution is unique [26].*

A.2 EQUILIBRIA

Of specific interest to this thesis is the long term behavior of dynamical systems, i.e. where the system ends up as $t \rightarrow \infty$. The dynamics of a system are determined by its equilibrium points.

Definition A.1. (Equilibrium Point) *An equilibrium point of Equation (A.1) is a point, $\bar{\mathbf{x}}$, such that $\frac{d\mathbf{x}}{dt} = \mathbf{f}(\bar{\mathbf{x}}) = 0$ [39].*

Equilibrium points, or fixed points, correspond to points in the domain of \mathbf{x} for which the system is not changing in time. There are two classifications of fixed points: hyperbolic and non-hyperbolic. This classification is based on the eigenvalues of the Jacobian matrix of Equation (A.1), $D\mathbf{f}(\mathbf{x})$, evaluated at the point.

Definition A.2. (Hyperbolic Fixed Point) *Let $\mathbf{x} = \bar{\mathbf{x}}$ be a fixed point of Equation (A.1). Then $\bar{\mathbf{x}}$ is called a hyperbolic fixed point if none of the eigenvalues of $D\mathbf{f}(\bar{\mathbf{x}})$ have zero real part [39].*

From Definition A.2 it is clear that a non-hyperbolic fixed point is one for which at least one of the eigenvalues has zero real part.

A.3 STABILITY

The stability of the equilibrium points of a dynamical system will further determine its dynamics. It is fairly straightforward to determine the stability of hyperbolic fixed points. Let \bar{x} be a hyperbolic fixed point of Equation (A.1). Then the associated linear vector field is given by the following:

$$\frac{d\xi}{dt} = Df(\bar{x})\xi, \quad \xi \in \mathbb{R}^n \quad (\text{A.2})$$

Theorem A.2. (Hartman-Grobman Theorem) *The flow generated by Equation (A.1) is topologically conjugate to the flow generated by Equation (A.2) in a neighborhood of the fixed point $x = \bar{x}$ [39].*

In the context of dynamical systems, if two systems are topologically conjugate, then their dynamics are qualitatively the same. The conclusion of Theorem A.2 implies that the local stability of a hyperbolic fixed point can be determined by the eigenvalues of the Jacobian evaluated at that point. An equilibrium point is locally stable if when the system experiences small perturbations from that point, it returns there. An equilibrium point is globally stable if all possible initial conditions have trajectories that move to that point.

Theorem A.3. *Suppose all of the eigenvalues of $Df(\bar{x})$ have negative real parts. Then the equilibrium point $x = \bar{x}$ of Equation (A.1) is asymptotically stable [39].*

Using Theorem A.3 it can be determined that an equilibrium point is unstable if at least one of the eigenvalues has positive real part.

A.4 TWO-DIMENSIONAL SYSTEMS

Some of the models studied in this thesis are two-dimensional, for which a further result can be obtained. A general two-dimensional nonlinear system is given below:

$$\begin{aligned} \dot{x} &= f(x, y) \\ \dot{y} &= g(x, y), \quad (x, y) \in \mathbb{R}^2 \end{aligned} \quad (\text{A.3})$$

where f and g are differentiable with continuous derivatives.

Theorem A.4. (Dulac's criterion) *Let $B(x, y)$ be a differentiable function with continuous derivatives on a simply connected region $D \subset \mathbb{R}^2$. If $\frac{\partial(Bf)}{\partial x} + \frac{\partial(Bg)}{\partial y}$ is not identically zero and does not change sign in D , then Equation (A.3) has no closed orbits lying entirely in D [39].*

Dulac's criterion is used to rule out closed orbits in a two-dimensional system.

APPENDIX B
LYTIC AND LYSOGENIC WORLDS

LYTIC AND LYSOGENIC WORLDS

This appendix contains the mathematical analysis that was performed for the lytic and lysogenic world models. These and all subsequent models will be left in terms of the original parameters. The results from these models are meant to be compared to environmental data that cannot be rescaled. Thus, while the common practice would be to non-dimensionalize the models, it is not necessary in this thesis.

B.1 LYTIC WORLD

A complete stability analysis of all equilibria in the lytic world model is performed. The model in question is given by Equation (2.1) and is reproduced below:

$$\begin{aligned}\frac{dM}{dt} &= r \left(1 - \frac{M}{K}\right) M - dMV, \\ \frac{dV}{dt} &= cdMV - mV.\end{aligned}\tag{B.1}$$

The meanings of the parameters used in Equation (B.1) are given in Table 2.1 in the main text. Note that the only parameter that is allowed to vary in this system is the carrying capacity of the bacteria, K .

B.1.1 Equilibria

Setting $\frac{dM}{dt} = \frac{dV}{dt} = 0$ and solving for M and V reveals that there are three combinations of bacteria and phage populations at which the lytic world is at equilibrium. The first is the trivial equilibrium and is given by $(M^*, V^*) = (0, 0)$. The second is given by $(M^*, V^*) = (K, 0)$. This equilibrium occurs when the system consists of only sensitive bacteria with no phages. Here in Equation (B.1) $\frac{dM}{dt}$ reduces to the logistic equation and thus there is an equilibrium at the carrying capacity, K [17]. The final equilibrium represents coexistence of the two populations and is given by the following:

$$(M^*, V^*) = \left(\frac{m}{cd}, \frac{r}{d} \left(1 - \frac{m}{cdK}\right)\right) = \left(M^*, \frac{r}{d} \left(1 - \frac{M^*}{K}\right)\right).\tag{B.2}$$

B.1.2 Stability

The behavior of the system will be determined by the stability of the equilibria. The goal here is to use the Hartman-Grobman Theorem (Theorem A.2) to determine the stability of each equilibrium point of the model. The Jacobian matrix of Equation (B.1) is given by the

following:

$$J|_{(M,V)} = \begin{pmatrix} r - \frac{2rM}{K} - dV & -dM \\ cdV & cdM - m \end{pmatrix}.$$

For the trivial equilibrium, $(M^*, V^*) = (0, 0)$, the Jacobian matrix evaluates to

$$J|_{(0,0)} = \begin{pmatrix} r & 0 \\ 0 & -m \end{pmatrix},$$

and the eigenvalues are $\lambda_1 = r$ and $\lambda_2 = -m$. Solutions will grow in one direction while decaying in the other direction, thus the trivial equilibrium can be classified as a saddle point and is unstable.

For the bacteria only equilibrium, $(M^*, V^*) = (K, 0)$, the Jacobian matrix evaluates to

$$J|_{(K,0)} = \begin{pmatrix} -r & -dK \\ 0 & cdK - m \end{pmatrix},$$

and the eigenvalues are $\lambda_1 = -r$ and $\lambda_2 = cdK - m$. While λ_1 remains negative, the sign of λ_2 changes from negative to positive at $K = \frac{m}{cd}$. The bacteria only equilibrium is thus stable when $K < \frac{m}{cd}$ and unstable when $K > \frac{m}{cd}$.

This change in stability and the fact that $\lambda_2 = 0$ implies that there is a bifurcation at $K = \frac{m}{cd}$. For the branch of fixed points, $(M^*, V^*) = (K, 0)$, it is always true that $V = 0$. Thus by setting $V = 0$ in Equation (B.1) the system simplifies to the following:

$$\frac{dM}{dt} = r \left(1 - \frac{M}{K} \right) M. \quad (\text{B.3})$$

Letting $x = \frac{r}{K}M$ Equation (B.3) can be written as

$$\frac{dx}{dt} = rx - x^2.$$

This is the normal form of a transcritical bifurcation [26]. This type of bifurcation occurs when two equilibrium points collide and exchange stability properties [39]. At $K = \frac{m}{cd}$, the bacteria-only equilibrium and the coexistence equilibrium, Equation (B.2), evaluate to the same expression. This implies that the two equilibrium points exchange stability here, which is verified below by determining the stability of the coexistence equilibrium.

For the coexistence equilibrium, Equation (B.2), the Jacobian matrix evaluates to

$$J|_{(M^*, V^*)} = \begin{pmatrix} -r\frac{M^*}{K} & -dM^* \\ cr\left(1 - \frac{M^*}{K}\right) & 0 \end{pmatrix},$$

and the eigenvalues are

$$\lambda_{1,2} = \frac{-rM^*}{2K} \pm \sqrt{\left(\frac{-rM^*}{2K}\right)^2 - mr\left(1 - \frac{M^*}{K}\right)}. \quad (\text{B.4})$$

When $K < \frac{m}{cd}$,

$$\left| \frac{-rM^*}{K} \right| < \sqrt{\left(\frac{-rM^*}{2K} \right)^2 - mr \left(1 - \frac{M^*}{K} \right)}.$$

Because all parameters are positive, this implies that $\lambda_{1,2} > 0$, and the equilibrium point is unstable. When $K > \frac{m}{cd}$

$$\left| \frac{-rM^*}{K} \right| > \sqrt{\left(\frac{-rM^*}{2K} \right)^2 - mr \left(1 - \frac{M^*}{K} \right)},$$

and $\text{Re}(\lambda_{1,2}) < 0$. It can be concluded that the equilibrium is locally stable for these values of K . Thus, the coexistence equilibrium is unstable when $K < \frac{m}{cd}$ and stable when $K > \frac{m}{cd}$. This corresponds to an exchange of stability properties with the bacteria only equilibrium at $K = \frac{m}{cd}$, verifying the existence of a transcritical bifurcation in the system.

Returning to the stability of Equation (B.2), it can be seen that when $K > \frac{m}{cd}$ there are different ways in which the system could return to this stable equilibrium if slightly perturbed. If $\left(\frac{-rM^*}{2K} \right)^2 > mr \left(1 - \frac{M^*}{K} \right)$, then the eigenvalues are real and negative thus the system is considered overdamped. The system returns to equilibrium quickly upon perturbation. On the other hand, if $\left(\frac{-rM^*}{2K} \right)^2 < mr \left(1 - \frac{M^*}{K} \right)$, then both eigenvalues are complex with negative real part and the system is considered underdamped. The system return to the equilibrium in an oscillatory fashion; the oscillations decrease as time increases. Lastly, if $\left(\frac{-rM^*}{2K} \right)^2 = mr \left(1 - \frac{M^*}{K} \right)$, then the eigenvalues are repeated and the system returns to equilibrium at a rate between that of the overdamped and underdamped cases. From a typical parameter sampling using a Latin Hypercube Sampling Scheme (see Appendix E) it is determined that when $K > \frac{m}{cd}$, $\lambda_{1,2}$ are complex with negative real part for $\approx 100\%$ of the parameter samples. The eigenvalues are real and negative very rarely and are never repeated. Thus, the system will exhibit dynamics of decaying oscillations as it returns to the coexistence equilibrium upon perturbation.

From a simple argument it can be shown that in this system the local stability of an equilibrium implies its global stability. To do this all other dynamics in the system are shown to be impossible. For this physical system it must be true that $M \geq 0$ and $V \geq 0$. The growth of the bacteria population is bounded by its carrying capacity, K . Because phages require bacteria to reproduce, the growth of the phage population is also bounded. Thus $M \not\rightarrow \infty$ and $V \not\rightarrow \infty$ as $t \rightarrow \infty$. The existence of closed orbits in this system can be ruled out. Let $\frac{dM}{dt} = f(M, V)$ and $\frac{dV}{dt} = g(M, V)$. Let S be a simply connected set such that

$$S = \{(M, V) \in \mathbb{R}_+^2\}.$$

If $B(M, V) = \frac{1}{MV}$, then

$$\frac{\partial(Bf)}{\partial M} + \frac{\partial(Bg)}{\partial V} = -\frac{r}{K} \frac{1}{V} < 0$$

By Dulac's Criterion (Theorem A.4) there are no closed orbits lying entirely inside S . The uniqueness of solutions also implies that there are no closed orbits along $M = 0$ or $V = 0$. Thus stable equilibria are globally stable in this system. All initial conditions have trajectories that move to $(M^*, V^*) = (K, 0)$ when $K < \frac{m}{cd}$ and to Equation (B.2) when $K > \frac{m}{cd}$.

The stability of the three equilibrium points in the system is summarized in Table B.1.

Table B.1. Summary of the Stability of All Equilibrium Points in the Lytic World Model

Equilibrium Point	Eigenvalues	Stability
$(M^*, V^*) = (0, 0)$	$\lambda_1 = r, \lambda_2 = -m$	unstable
$(M^*, V^*) = (K, 0)$	$\lambda_1 = -r, \lambda_2 = cdK - m$	unstable when $K > \frac{m}{cd}$, stable when $K < \frac{m}{cd}$
$(M^*, V^*) = \left(\frac{m}{cd}, \frac{r}{d} \left(1 - \frac{M^*}{K}\right)\right)$	Equation (B.4)	stable when $K > \frac{m}{cd}$

B.2 LYSOGENIC WORLD

A complete stability analysis of all equilibria in the lysogenic world model is performed. The model in question is given by Equation (2.6) and it is reproduced below:

$$\begin{aligned} \frac{dL}{dt} &= r \left(1 - \frac{L}{K}\right) L - \beta L, \\ \frac{dT}{dt} &= c\beta L - mT - \chi dLT. \end{aligned} \tag{B.5}$$

The meanings of the parameters used in Equation (B.5) are given in Table 2.2 in the main text. Note that the only parameter that is allowed to vary in this system is the carrying capacity of the lysogens, K .

B.2.1 Equilibria

Setting $\frac{dL}{dt} = \frac{dT}{dt} = 0$ and solving for L and T reveals that there are two combinations of lysogen and phage populations at which the lysogenic world is at equilibrium. The first is the trivial equilibrium, $(L^*, T^*) = (0, 0)$, and the second represents coexistence in the system and is given below:

$$(L^*, T^*) = \left(\left(1 - \frac{\beta}{r}\right) K, \frac{c\beta \left(1 - \frac{\beta}{r}\right) K}{m + \chi d \left(1 - \frac{\beta}{r}\right) K} \right) = \left(L^*, \frac{c\beta L^*}{m + \chi d L^*} \right). \tag{B.6}$$

B.2.2 Stability

The Hartman-Grobman Theorem (Theorem A.2) is used to determine the stability of each equilibrium point of the model. The Jacobian matrix of Equation (B.5) is given by the

following:

$$J|_{(L,T)} = \begin{pmatrix} r - \frac{2rL}{K} - \beta & 0 \\ c\beta - \chi dT & -m - \chi dL \end{pmatrix}.$$

For the trivial equilibrium, $(L^*, T^*) = (0, 0)$, the Jacobian matrix evaluates to

$$J|_{(L^*, T^*)} = \begin{pmatrix} r - \beta & 0 \\ c\beta & -m \end{pmatrix},$$

and the eigenvalues are $\lambda_1 = r - \beta$ and $\lambda_2 = -m$. While λ_2 remains negative, the sign of λ_1 depends on the values of r and β . The trivial equilibrium is locally stable when $r < \beta$ and unstable when $r > \beta$.

For the coexistence equilibrium, Equation (B.6), the Jacobian matrix evaluates to

$$J|_{(L^*, T^*)} = \begin{pmatrix} \beta - r & 0 \\ c\beta - \chi dT^* & -m - \chi d \left(1 - \frac{\beta}{r}\right) K \end{pmatrix},$$

and the eigenvalues are given by $\lambda_1 = \beta - r$ and $\lambda_2 = -m - \chi d \left(1 - \frac{\beta}{r}\right) K$. When $r < \beta$, $\lambda_1 > 0$ making this equilibrium unstable. When $r > \beta$, both λ_1 and λ_2 are negative implying that the equilibrium is locally stable.

Note that the change in stability between the two equilibrium points implies that there is a bifurcation at $r = \beta$. Specifically, there is a transcritical bifurcation because the trivial and coexistence equilibrium points evaluate to the same expression at $r = \beta$ and exchange stability here. However, the values of r and β given in Table 2.2 reveal that $r \gg \beta$. Thus while a bifurcation occurs in the mathematical model, it is not expected in the physical system.

Using an argument similar to that used in Appendix B.1.2 it can be shown that the local stability of an equilibrium point implies its global stability. To do this all other dynamics in the system are shown to be impossible. For this physical system it must be true that $L \geq 0$ and $T \geq 0$. The growth of the lysogen population is bounded by the carrying capacity of the system. Temperate phages are only introduced into the system when lysogens lyse, thus the growth of the phage population is bounded as well. From this it can be seen that as $t \rightarrow \infty$, $L \not\rightarrow \infty$ and $T \not\rightarrow \infty$. The system may contain a closed orbit that could attract trajectories. To rule out closed orbits in this system let $\frac{dL}{dt} = f(L, T)$ and $\frac{dT}{dt} = g(L, T)$. Let S be a simply connected set such that

$$S = \{(L, T) \in \mathbb{R}_+^2\}.$$

Let $B(L, T) = \frac{1}{LT}$, then

$$\frac{\partial(Bf)}{\partial L} + \frac{\partial(Bg)}{\partial T} = -\frac{r}{K} \frac{1}{T} - \frac{c\beta}{T^2} < 0$$

By Dulac's Criterion (Theorem A.4) there are no closed orbits lying entirely inside S . The uniqueness of solutions also implies that there are no closed orbits along $L = 0$ or $T = 0$. Thus stable equilibria are globally stable in this system. All initial conditions will move to $(L^*, T^*) = (0, 0)$ when $r < \beta$ and Equation (B.6) when $r > \beta$. The stability of the two equilibrium points in the system are summarized in Table B.2.

Table B.2. Summary of the Stability of All Equilibrium Points in the Lysogenic World Model

Equilibrium Point	Eigenvalues	Stability
$(L^*, T^*) = (0, 0)$	$\lambda_1 = r - \beta, \lambda_2 = -m$	stable when $r < \beta$ unstable when $r > \beta$
$(L^*, T^*) = \left(L^*, \frac{c\beta L^*}{m + \chi d L^*}\right)$	$\lambda_1 = \beta - r, \lambda_2 = -m - \chi d \left(1 - \frac{\beta}{r}\right) K$	unstable when $r < \beta$ stable when $r > \beta$

B.2.3 Effect of χ on the Lysogenic World Model

The value of χ determines a transition in the behavior of T^* in Equation (B.6) as a function of K . Recall that the expression for T^* is given by the following:

$$T^* = \frac{c\beta \left(1 - \frac{\beta}{r}\right) K}{m + \chi d \left(1 - \frac{\beta}{r}\right) K}.$$

For $m \gg \chi d \left(1 - \frac{\beta}{r}\right) K$, the expression for T^* can be approximated by

$$T^* \approx \frac{c\beta \left(1 - \frac{\beta}{r}\right)}{m} K.$$

Here T^* grows linearly with K .

For $m \ll \chi d \left(1 - \frac{\beta}{r}\right) K$, the expression for T^* can now be approximated by

$$T^* \approx \frac{c\beta}{\chi d}.$$

Here T^* is constant in K .

The observed transition occurs when

$$m \sim \chi d \left(1 - \frac{\beta}{r}\right) K. \quad (\text{B.7})$$

Let $\bar{K} \sim 10^n$ represent the value K for which this transition occurs. Also let $\chi = 10^{-y}$ for $\chi \in (0, 1]$. The baseline parameter values used in the Latin Hypercube Sampling Scheme

(Appendix E) imply $m \sim 10^{-1}$, $d \sim 10^{-8}$, and $(1 - \frac{\beta}{r}) \sim 1$. Taking the logarithm of Equation (B.7) and using the above stated values

$$\begin{aligned} \log(m) &\sim \log(\chi) + \log(d) + \log\left(1 - \frac{\beta}{r}\right) + \log(\overline{K}) \\ \log(10^{-1}) &\sim \log(10^{-y}) + \log(10^{-8}) + \log(10^n) \\ n &\sim 7 + y \end{aligned} \tag{B.8}$$

Thus for $\chi > 0$, the value of χ will determine a change in the behavior of T^* as a function of K .

APPENDIX C
MIXED WORLDS INCLUDING BOTH
VIRULENT AND TEMPERATE PHAGES

MIXED WORLDS INCLUDING BOTH VIRULENT AND TEMPERATE PHAGES

This appendix contains the mathematical analysis that was performed for the mixed world models.

C.1 TEMPERATE PHAGES CHOOSE LYTIC LIFESTYLE

A complete stability analysis of all equilibria in the mixed world model where temperate phages always choose the lytic lifestyle is performed. The model in question is given by Equation (3.1) and is reproduced below:

$$\begin{aligned}\frac{dM}{dt} &= r \left(1 - \frac{N}{K}\right) M - dMV - dMT, \\ \frac{dV}{dt} &= cdMV - mV, \\ \frac{dT}{dt} &= cdMT - mT.\end{aligned}\tag{C.1}$$

The meanings of the parameters used in Equation (C.1) are given in Table 3.1 in the main text. Note that the only parameter that varies in this system is the carrying capacity of the bacteria, K .

C.1.1 Equilibria

Setting $\frac{dM}{dt} = \frac{dV}{dt} = \frac{dT}{dt} = 0$ and solving for M , V , and T reveals that there are three combinations of bacteria and phage populations at which this system is at equilibrium. The first is the trivial equilibrium, $(M^*, V^*, T^*) = (0, 0, 0)$. The second corresponds to a system in which only bacteria survive and is given by $(M^*, V^*, T^*) = (K, 0, 0)$. The final equilibrium is one of coexistence between all three populations and is given below:

$$(M^*, P^*) = \left(\frac{m}{cd}, \frac{r}{d} \left(1 - \frac{m}{cdK}\right)\right) = \left(M^*, \frac{r}{d} \left(1 - \frac{M^*}{K}\right)\right),\tag{C.2}$$

where $P^* = V^* + T^*$.

The distribution of the phage species can be determined from the ratio of $\frac{dV}{dt}$ and $\frac{dT}{dt}$, which leads to the following differential equation:

$$\frac{dV}{dP} = \frac{(cdM - m)V}{(cdM - m)P} = \frac{V}{P}.$$

Separating variables and letting the initial condition of the system be $V(t_0) = V_0$ and $P(t_0) = P_0$, the solution is

$$\frac{V(t)}{P(t)} = \frac{V_0}{P_0} .$$

This equation implies that the ratio of V and P will remain constant in the system. Letting $T(t_0) = T_0$ and using a similar argument as above it can be seen that

$$\frac{T(t)}{P(t)} = \frac{T_0}{P_0} .$$

Thus, the distribution of phage species remains constant for all time, t , and is determined by the initial distribution of the species.

C.1.2 Stability

Given the results from the previous section it is seen to be more convenient to study the dynamics of the total phage population, P , and bacteria population, M . Equation (C.1) is rewritten below accordingly:

$$\begin{aligned} \frac{dM}{dt} &= r \left(1 - \frac{N}{K} \right) M - dMP , \\ \frac{dP}{dt} &= cdMP - mP . \end{aligned} \tag{C.3}$$

Here the lytic world has been recovered and all further analysis is identical to that completed in Section B.1.2.

C.2 TEMPERATE PHAGES CHOOSE LYSOGENIC LIFESTYLE

A stability analysis of equilibria in the model describing the interaction of a single species of sensitive bacteria, virulent phages, lysogens, and temperate phages that choose the lysogenic lifestyle is performed. The model in question is given by Equation (3.4) and is reproduced below:

$$\begin{aligned} \frac{dM}{dt} &= r \left(1 - \frac{N}{K} \right) M - dMV - dMT + sL , \\ \frac{dV}{dt} &= cdMV - \chi dVL - mV , \\ \frac{dL}{dt} &= r \left(1 - \frac{N}{K} \right) L - \beta L + dMT - sL , \\ \frac{dT}{dt} &= c\beta L - \chi dTL - dMT - mT . \end{aligned} \tag{C.4}$$

The meanings of the parameters used in Equation (C.4) are given in Table 3.1 in the main text. Note that the only parameter that varies in this system is the carrying capacity of the sensitive bacteria and lysogens, K .

C.2.1 Equilibria

Setting $\frac{dM}{dt} = \frac{dV}{dt} = \frac{dL}{dt} = \frac{dT}{dt} = 0$ and solving for M , V , L , and T reveals that there are five combinations of populations for which the system is at equilibrium. The first is the trivial equilibrium and is given by $(M^*, V^*, L^*, T^*) = (0, 0, 0, 0)$. The second is given by $(M^*, V^*, L^*, T^*) = (K, 0, 0, 0)$ and represents a system in which only sensitive bacteria are able to survive. The third is the lytic world equilibrium, $(M^*, V^*, L^*, T^*) = (\frac{m}{cd}, \frac{r}{d} (1 - \frac{m}{cdK}), 0, 0)$, referred to as such because it recovers the coexistence equilibrium of the lytic world. Another equilibrium occurs at a point when only sensitive bacteria, lysogens, and temperate phages exist in the system. The fifth and final equilibrium point represents coexistence of all four populations in the system and is given by the following expressions:

$$M^* = \frac{m}{cd} + \frac{\chi}{c} L^*, \quad (C.5)$$

$$V^* = \frac{r}{d} \left(1 - \frac{N^*}{K} \right) + \frac{s}{d} \frac{L^*}{M^*} - T^*, \quad (C.6)$$

$$L^* = \frac{c}{c + \chi} \left(\left(1 - \frac{\beta}{r(1+c)} - \frac{s}{r} \right) K - \frac{m}{cd} \right), \quad (C.7)$$

$$T^* = \left(\frac{\beta + s}{d} - \frac{r}{d} \left(1 - \frac{N^*}{K} \right) \right) \frac{L^*}{M^*}. \quad (C.8)$$

C.2.2 Stability

The local stability of each equilibrium point is determined using Theorem A.2. The Jacobian matrix of Equation (C.4) is given by the following:

$$J = \begin{pmatrix} r - \frac{2rM}{K} - \frac{rL}{K} - dV - dT & -dM & -\frac{rM}{K} + s & -dM \\ cdV & cdM - m - \chi dL & -\chi dV & 0 \\ -\frac{rL}{K} + dT & 0 & r - \frac{2rL}{K} - \frac{rM}{K} - \beta - s & dM \\ -dT & 0 & c\beta - \chi dT & -m - \chi dL - dM \end{pmatrix}.$$

For the trivial equilibrium, $(M^*, V^*, L^*, T^*) = (0, 0, 0, 0)$

$$J|_{(0,0,0,0)} = \begin{pmatrix} r & 0 & s & 0 \\ 0 & -m & 0 & 0 \\ 0 & 0 & r - \beta - s & 0 \\ 0 & 0 & c\beta & -m \end{pmatrix},$$

and the eigenvalues of this matrix are $\lambda_1 = r$, $\lambda_2 = -m$, $\lambda_3 = r - \beta - s$, and $\lambda_4 = -m$. Because $\lambda_1 > 0$ this implies that the trivial equilibrium is always unstable.

For the sensitive bacteria only equilibrium, $(M^*, V^*, L^*, T^*) = (K, 0, 0, 0)$

$$J|_{(K,0,0,0)} = \begin{pmatrix} -r & -dK & -r+s & -dK \\ 0 & cdK-m & 0 & 0 \\ 0 & 0 & -\beta-s & dK \\ 0 & 0 & c\beta & -m-dK \end{pmatrix},$$

and the eigenvalues of this matrix are $\lambda_1 = -r$, $\lambda_2 = cdK - m$,

$$\lambda_{3,4} = \frac{1}{2} \left(-(\beta + s + m + dK) \pm \sqrt{(\beta + s + m + dK)^2 - 4((\beta + s)(m + dK) - c\beta dK)} \right).$$

It is clear that $\lambda_1 < 0$. The sign of λ_2 depends on the value of K and determines the stability of this equilibrium. When $K < \frac{m}{cd}$ then $\lambda_2 < 0$ and

$$|-(\beta + s + m + dK)| > \sqrt{(\beta + s + m + dK)^2 - 4((\beta + s)(m + dK) - c\beta dK)},$$

which implies that $\text{Re}(\lambda_3, \lambda_4) < 0$. Thus this equilibrium is stable. When $K > \frac{m}{cd}$ then $\lambda_2 > 0$ and the equilibrium is unstable. When the sensitive bacteria only equilibrium is stable the system reduces to Equation (B.3), and using the same justification as Section B.1.2, it can be shown that this system undergoes a transcritical bifurcation at $K_0 = \frac{m}{cd}$.

For the lytic world equilibrium $(M, V, L, T) = (\frac{m}{cd}, \frac{r}{d} (1 - \frac{M}{K}), 0, 0)$

$$J|_{(M^*, V^*, 0, 0)} = \begin{pmatrix} -\frac{rm}{cdK} & -\frac{m}{c} & -\frac{rm}{cdK} + s & -\frac{m}{c} \\ rc(1 - \frac{m}{cdK}) & 0 & -r(1 - \frac{m}{cdK}) & 0 \\ 0 & 0 & r - \frac{rm}{cdK} - \beta - s & \frac{m}{c} \\ 0 & 0 & c\beta & -m - \frac{m}{c} \end{pmatrix}.$$

The first two eigenvalues of this matrix are given by

$$\lambda_{1,2} = -\frac{rM^*}{2K} \pm \sqrt{\left(\frac{rM^*}{2K}\right)^2 - m\left(1 - \frac{M^*}{K}\right)},$$

and the second two given by

$$\lambda_{3,4} = \frac{1}{2} \left(r - \frac{rm}{cdK} - \beta - s - m - \frac{m}{c} \right) \pm \sqrt{\left(\frac{1}{2} \left(r - \frac{rm}{cdK} - \beta - s - m - \frac{m}{c} \right)\right)^2 + rm\left(1 - \frac{m}{cdK}\right)\left(\frac{c+1}{c}\right) - \frac{\beta m}{c} - sm\left(\frac{c+1}{c}\right)}.$$

The signs of $\lambda_{1,2}$ have previously been discussed when they arose in the lytic world. When $K < \frac{m}{cd}$, $\lambda_{1,2} > 0$ and the equilibrium is unstable. When $K > \frac{m}{cd}$ it can be determined that the quantity under the square root in $\lambda_{3,4}$ is positive using $r \gg \beta, s$. At least one of these eigenvalues will be positive, and thus the lytic world equilibrium is unstable for all values of K .

The equilibrium when only sensitive bacteria, lysogens, and temperate phages exist in the system is found numerically. An optimization approach is used to solve for the solution of the system of three nonlinear equations that arises. Samples of initial conditions are created using a Latin Hypercube Sampling Scheme (Appendix E) over relevant ranges for each variable. The optimization algorithm is implemented in MATLAB and uses a trust region search with a dogleg step [19]. Different initial conditions are tested until the stable equilibrium solution is found. Stability is determined by evaluating the Jacobian matrix at the solution and numerically finding its eigenvalues. Through experimentation, it is determined that the sensitive bacteria, lysogen, and temperate phage equilibrium is very rarely stable in this system ($\approx 4\%$ of the samples when $K > \frac{m}{cd}$). The algorithm is therefore only called when all other equilibria are determined to be unstable.

The stability of the coexistence equilibrium is analyzed by evaluating the Jacobian matrix at the equilibrium and numerically finding its eigenvalues. Experimentation lead to the conclusion that the coexistence equilibrium is stable for $\approx 96\%$ of the samples when $K > \frac{m}{cd}$.

C.2.3 Effect of χ

The effect of the immunity of the lysogens on the dynamics of this system is studied. The lysogen population is able to grow linearly with K as seen in Equation (C.7). Thus once lysogens enter the system there will be some carrying capacity, \tilde{K} , for which the value of $\frac{\chi}{c}L^*$ dominates in the expression for M^* (Equation (C.5)). This will initiate a transition in the behavior of the sensitive bacteria from being controlled by the phages to growing linearly with K . Assume that K is large enough so that $L^* \sim \tilde{K}$. This transition will then occur when

$$\frac{m}{cd} \sim \frac{\chi}{c} \tilde{K}. \quad (\text{C.9})$$

Let $\tilde{K} \sim 10^n$ and let $\chi = 10^{-y}$ for $\chi \in (0, 1]$. The baseline parameter values used in the Latin Hypercube Sampling Scheme (Appendix E) imply $m \sim 10^{-1}$, $c \sim 10^1$, and $d \sim 10^{-8}$. Taking the logarithm of Equation (C.9) and using order of magnitudes of the parameters

$$\begin{aligned} \log\left(\frac{m}{cd}\right) &\sim \log(\chi) - \log(c) + \log(\tilde{K}) \\ \log\left(\frac{10^{-1}}{10^1 10^{-8}}\right) &\sim \log(10^{-y}) - \log(10^1) + \log(10^n) \end{aligned}$$

$$n \sim 7 + y \quad (\text{C.10})$$

This result implies that the value of χ determines when the transition in the behavior of the sensitive bacteria population as a function of K will occur.

C.3 TEMPERATE PHAGES HAVE LIFESTYLE DECISION

A stability analysis of equilibria in the model describing the interaction of a single species of sensitive bacteria, virulent phages, lysogens, and temperate phages which have a lifestyle decision is performed. The model in question is given by Equation (3.10) and is reproduced below:

$$\begin{aligned} \frac{dM}{dt} &= r \left(1 - \frac{N}{K} \right) M - dMV - dMT + sL, \\ \frac{dV}{dt} &= cdMV - \chi dVL - mV, \\ \frac{dL}{dt} &= r \left(1 - \frac{N}{K} \right) L - \beta L + fdMT - sL, \\ \frac{dT}{dt} &= c\beta L - \chi dTL - fdMT + (1 - f)cdMT - mT. \end{aligned} \quad (\text{C.11})$$

The meanings of the parameters used in Equation (C.11) are given in Table 3.1 in the main text. Note that the only parameter that varies in this system is K , the carrying capacity of the sensitive bacteria and lysogens.

C.4 EQUILIBRIA

Setting $\frac{dM}{dt} = \frac{dV}{dt} = \frac{dL}{dt} = \frac{dT}{dt} = 0$ and solving for M , V , L , and T reveals that there five combinations of populations for which the system is at equilibrium. The first is the trivial equilibrium and is given by $(M^*, V^*, L^*, T^*) = (0, 0, 0, 0)$. The second is given by $(M^*, V^*, L^*, T^*) = (K, 0, 0, 0)$ and represents a system in which there are only sensitive bacteria with no predators. The third is the lytic world equilibrium, $(M^*, V^*, L^*, T^*) = \left(\frac{m}{cd}, \frac{r}{d} \left(1 - \frac{m}{cdK} \right), 0, 0 \right)$, referred to as such because it recovers the coexistence equilibrium of the lytic world. Another equilibrium occurs when when only sensitive bacteria, lysogens, and temperate phages exist in the system. The fifth and final equilibrium point represents coexistence of all four populations in the system and is given by the following expressions:

$$M^* = \frac{A + \sqrt{B}}{2rcd(f - 1)}, \quad (\text{C.12})$$

$$V^* = \frac{r}{d} \left(1 - \frac{N^*}{K}\right) + \frac{s}{d} \frac{L^*}{M^*} - T^*, \quad (\text{C.13})$$

$$L^* = \frac{(r-s)cdK - rm}{rd(c+\chi)}, \quad (\text{C.14})$$

$$T^* = \left(\frac{\beta+s}{fd} - \frac{r}{fd} \left(1 - \frac{N^*}{K}\right) \right) \frac{L^*}{M^*}, \quad (\text{C.15})$$

where

$$A = \beta cdK - cd(f-1)(rL^* + (s-r)K) - r(m + \chi dL^*),$$

and

$$\begin{aligned} B &= (\beta cdK)^2 + (cd(f-1)(rK - rL^* - sK) + r(m + \chi dL^*))^2 \\ &\quad + 2\beta cdK(cd(f-1)(rK - rL^* - sK) - (2f-1)r(m + \chi dL^*)). \end{aligned}$$

C.5 STABILITY

The local stability of each equilibrium point is determined using Theorem A.2. The Jacobian matrix of Equation C.11 is given by the following:

$$J = \begin{pmatrix} r - \frac{2rM}{K} - \frac{rL}{K} - dV - dT & -dM & -\frac{rM}{K} + s & -dM \\ cdV & cdM - m - \chi dL & -\chi dV & 0 \\ -\frac{rL}{K} + fdT & 0 & r - \frac{2rL}{K} - \frac{rM}{K} - \beta - s & fdM \\ -fdT + (1-f)cdT & 0 & c\beta - \chi dT & -m - \chi dL - fdM + (1-f)cdM \end{pmatrix}.$$

For the trivial equilibrium, $(M^*, V^*, L^*, T^*) = (0, 0, 0, 0)$

$$J|_{(0,0,0,0)} = \begin{pmatrix} r & 0 & s & 0 \\ 0 & -m & 0 & 0 \\ 0 & 0 & r - \beta - s & 0 \\ 0 & 0 & c\beta & -m \end{pmatrix},$$

and the eigenvalues of this matrix are $\lambda_1 = r$, $\lambda_2 = -m$, $\lambda_3 = r - \beta - s$, and $\lambda_4 = -m$. Because $\lambda_1 > 0$ this implies that the trivial equilibrium is unstable.

For the sensitive bacteria only equilibrium, $(M^*, V^*, L^*, T^*) = (K, 0, 0, 0)$

$$J|_{(K,0,0,0)} = \begin{pmatrix} -r & -dK & -r + s & -dK \\ 0 & cdK - m & 0 & 0 \\ 0 & 0 & -\beta - s & fdK \\ 0 & 0 & c\beta & -m - fdK + (1-f)cdK \end{pmatrix},$$

and the eigenvalues of this matrix are $\lambda_1 = -r$, $\lambda_2 = cdK - m$,

$$\lambda_{3,4} = \frac{1}{2} \left(-(\beta + s + m + fdK - cdK(1 - f)) \right. \\ \left. \pm \sqrt{(\beta + s + m + fdK - cdK(1 - f))^2 - 4((\beta + s)(m - cdK) + (sc + \beta + 1)fdK)} \right).$$

It is clear that $\lambda_1 < 0$. The sign of λ_2 depends on the value of K and determines the stability of this equilibrium. When $K < \frac{m}{cd}$ then $\lambda_2 < 0$ and

$$| -(\beta + s + m + fdK - cdK(1 - f)) | > \sqrt{(\beta + s + m + fdK - cdK(1 - f))^2 - 4((\beta + s)(m - cdK) + (sc + \beta + 1)fdK)},$$

which implies that $\text{Re}(\lambda_3, \lambda_4) < 0$. Thus this equilibrium is stable. When $K > \frac{m}{cd}$ then $\lambda_2 > 0$ and the equilibrium is unstable. When the sensitive bacteria only equilibrium is stable the system reduces to Equation (B.3) and using the same justification as Section B.1.2, it can be shown that this system undergoes a transcritical bifurcation at $K_0 = \frac{m}{cd}$.

The stability of the lytic world equilibrium and coexistence equilibrium is analyzed numerically as described in Appendix C.2.2. The lytic world equilibrium is found to never be stable and the stability of the coexistence equilibrium is found to depend on the value of f .

The stability of the equilibrium when only sensitive bacteria, lysogens, and temperate phages exist in the system is determined for this model in the same way as described in Appendix C.2.2. The stability of this equilibrium is found to depend on the value of f .

APPENDIX D
COMMUNITY WORLDS

COMMUNITY WORLDS

This appendix contains the mathematical analysis that was performed for the lytic and lysogenic community world models.

D.1 LYTIC COMMUNITY WORLD

A stability analysis of all equilibria in the lytic community world is performed. The model in question is given by Equation (4.1) and is reproduced below:

$$\begin{aligned}\frac{dM_i}{dt} &= r \left(1 - \frac{M}{K} \right) M_i - dM_i V_i, \\ \frac{dV_i}{dt} &= cdM_i V_i - mV_i,\end{aligned}\tag{D.1}$$

where $i = 1, 2, \dots, n$.

D.1.1 Equilibria

Setting $\frac{dM_i}{dt} = \frac{dV_i}{dt} = 0$ and solving for M_i and V_i reveals that there are three combinations of populations of bacteria and phage species for which the system is at equilibrium. The first equilibrium is the trivial equilibrium, given by $(M_i^*, V_i^*) = (0, 0)$. The next is an extension of the bacteria only equilibrium from the single species model and is given by $(M^*, V^*) = (K, 0)$. Here the community of bacteria grows to the system's carrying capacity, and concentrations for individual species of bacteria are not explicit.

The distribution of the bacteria species can be determined from the ratio of $\frac{dM_i}{dt}$ and $\frac{dM}{dt}$, which leads to the following differential equation:

$$\frac{dM_i}{dM} = \frac{r \left(1 - \frac{M}{K} \right) M_i}{r \left(1 - \frac{M}{K} \right) M} = \frac{M_i}{M}.$$

Separating variables and letting the initial condition of the system be $M_i(t_0) = M_{i0}$ and $M(t_0) = M_0$, the solution is given by

$$\frac{M_i(t)}{M(t)} = \frac{M_{i0}}{M_0}.$$

This equation implies that the ratio of M_i and M will remain constant in time, and thus the distribution of bacteria species is determined by the initial conditions of the system.

The third equilibrium is an extension of the coexistence equilibrium in the single species system. It is given by the following expressions:

$$M_i^* = \frac{m}{cd},\tag{D.2}$$

$$V_i^* = \frac{r}{d} \left(1 - \frac{mn}{cdK}\right) = \frac{r}{d} \left(1 - n \frac{M_i^*}{K}\right). \quad (\text{D.3})$$

The expression for the population of the bacteria community at this equilibrium is attained by summing over all species of bacteria.

$$M^* = \sum_{i=1}^n \frac{m}{cd} = n \frac{m}{cd} = n \cdot M_i^*. \quad (\text{D.4})$$

Similarly, the expression for the population of the phage community can be attained by summing over all species of phage.

$$V^* = \sum_{i=1}^n \frac{r}{d} \left(1 - \frac{mn}{cdK}\right) = \frac{rn}{d} \left(1 - \frac{mn}{cdK}\right) = \frac{rc}{m} M^* \left(1 - \frac{M^*}{K}\right). \quad (\text{D.5})$$

D.1.2 Stability

The Jacobian matrix of Equation (D.1) is given by the following:

$$J|_{(M_i, V_i)} = \left(\begin{array}{cccccc|cccc} r - \frac{rM}{K} - \frac{rM_1}{K} - dV_1 & -\frac{rM_1}{K} & \cdots & \cdots & \cdots & -\frac{rM_1}{K} & -dM_1 & \cdots & 0 \\ -\frac{rM_2}{K} & \ddots & & & & \vdots & \ddots & & \\ \vdots & & r - \frac{rM}{K} - \frac{rM_i}{K} - dV_i & & & \vdots & & -dM_i & \\ \vdots & & & \ddots & & -\frac{rM_{n-1}}{K} & & \ddots & \\ -\frac{rM_n}{K} & & & & r - \frac{rM}{K} - \frac{rM_n}{K} - dV_n & 0 & & & -dM_n \\ \hline & cdV_1 & & 0 & & 0 & cdM_1 - m & & 0 \\ & & \ddots & & & & \ddots & & \\ & & & cdV_i & & & & cdM_i - m & \\ & & & & \ddots & & & \ddots & \\ & 0 & & & & cdV_n & 0 & & cdM_n - m \end{array} \right).$$

For the trivial equilibrium, $(M_i^*, V_i^*) = (0, 0)$, the Jacobian matrix evaluates to the following:

$$J|_{(0,0)} = \left(\begin{array}{ccc|ccc} \ddots & r & 0 & \mathbf{0} & & \\ 0 & \ddots & & & \mathbf{0} & \\ \mathbf{0} & & & \ddots & -m & 0 \\ & & & 0 & & \ddots \end{array} \right),$$

and the eigenvalues are given by $\lambda_i = r$ for $i = 1, \dots, n$ and $\lambda_i = -m$ for $i = n + 1, \dots, 2n$. Applying Theorem A.2 implies that the trivial equilibrium is always unstable.

For the bacteria only equilibrium, $(M^*, V^*) = (K, 0)$ the Jacobian matrix evaluates to the following:

$$J|_{(M^*, V^*)} = \left(\begin{array}{cccc|cccc} -\frac{rM_1^*}{K} & \frac{-rM_1^*}{K} & \dots & \dots & \frac{-rM_1^*}{K} & -dM_1^* & & 0 \\ -\frac{rM_2^*}{K} & \ddots & & & \vdots & \ddots & & \\ \vdots & & \frac{-rM_i^*}{K} & & \vdots & & -dM_i^* & \\ \vdots & & & \ddots & \frac{-rM_{n-1}^*}{K} & & \ddots & \\ -\frac{rM_n^*}{K} & & & & \frac{-rM_n^*}{K} & 0 & & -dM_n^* \\ \hline & & & & & cdM_1^* - m & & 0 \\ & & & & & \ddots & & \\ & & & & & & cdM_i^* - m & \\ & & & & & & \ddots & \\ & & & & & 0 & & cdM_n^* - m \end{array} \right).$$

The $2n$ eigenvalues of this matrix are $\lambda = -r$, $n - 1$ copies of $\lambda = 0$, and $\lambda = cdM_i - m$ for $i = 1, \dots, n$. This equilibrium is therefore non-hyperbolic and Theorem A.2 cannot be applied to determine its stability.

For the coexistence equilibrium, $(M_i^*, V_i^*) = \left(\frac{m}{cd}, \frac{r}{d} \left(1 - \frac{mn}{cdK}\right)\right)$, using $M^* = \frac{mn}{cdK}$ the Jacobian matrix evaluates to the following:

$$J|_{(M_i^*, V_i^*)} = \left(\begin{array}{ccc|ccc} & \ddots & \frac{-rm}{cdK} & \ddots & & 0 \\ & & \frac{-rm}{cdK} & & -\frac{m}{c} & \\ \frac{-rm}{cdK} & & \ddots & 0 & \ddots & \\ \ddots & & & 0 & & \\ & rc \left(1 - \frac{mn}{cdK}\right) & & & \mathbf{0} & \\ 0 & & \ddots & & & \end{array} \right).$$

The $2n$ eigenvalues of this matrix are

$$\lambda = -\frac{rM^*}{2K} \pm \sqrt{\left(\frac{rM^*}{2K}\right)^2 - rm \left(1 - \frac{M^*}{K}\right)},$$

and $n - 1$ copies of

$$\lambda = \pm i \sqrt{rm \left(1 - \frac{mn}{cdK}\right)} = \pm i \sqrt{rm \left(1 - \frac{M^*}{K}\right)}.$$

Of these eigenvalues $2n - 2$ of them have $\text{Re}(\lambda) = 0$, thus the coexistence equilibrium is non-hyperbolic and Theorem A.2 cannot be applied to determine its stability.

While the standard process to analyze the stability of hyperbolic equilibria is to perform a center manifold reduction, a numerical approach is chosen instead. For the purposes of this thesis a numerical approximation of stability is satisfactory.

This community model is an extension of the lytic world. This leads to the prediction that when $K < \frac{mn}{cd}$ the bacteria only equilibrium will be stable and when $K > \frac{mn}{cd}$ the coexistence equilibrium will be stable. To test this hypothesis MATLAB's ode45 solver is utilized. Simulations are run for $K = 10^5, 10^6, 10^7$, and 10^8 . For each value of K , 10^3 parameter samples are created using a Latin Hypercube Sampling Scheme (Appendix E). For each parameter sample Equation (D.1) is solved over a large time span ($t \in [0, 5 \times 10^4]$ hours). The stability of the equilibrium is identical for all $n > 1$, thus a community with $n = 2$ is chosen to save computation time. The eigenvalues corresponding to the coexistence equilibrium indicate that there are oscillatory dynamics in the system. To account for this the bacteria and phage community concentrations are averaged over a range of times in the interval. A kernel probability distribution is then fit to these averages for each value of K . These probability distributions are given in Figure D.1.

To compare the probability distributions to the predicted stable equilibrium points, 10^3 parameter samples are created using the Latin Hypercube Sampling Scheme (Appendix E) and the average value for each parameter is calculated. The values of Equation (D.4) and (D.5) using the average parameter values are plotted on the x -axis in Figure D.1 as red and green data points, respectively. The value of the bacteria community for the bacteria only equilibrium is also plotted along the x -axis as a black data point.

Figure D.1 (a) corresponds to $K = 10^5$ and here it can be observed that the majority of the samples stabilize at the bacteria only equilibrium. This aligns with the prediction that for small values of carrying capacity the phage community will become extinct and the bacteria community would grow to K . Panels (b) and (c) correspond to the bacteria and phage community for $K = 10^6$, respectively. Most simulations return values near the predicted value for the bacteria coexistence equilibrium with a few stabilizing at the bacteria only equilibrium. This is to be expected as around this value of K the system is undergoing a transition between the two different states. The simulations return values that are shifted from the predicted phage coexistence equilibrium value. This corresponds to a mix of values between the coexistence equilibrium and the bacteria-only equilibrium at which the phage community is zero. Panels (d) and (e) correspond to the bacteria and phage community for $K = 10^7$, respectively. A similar behavior to the simulations from $K = 10^6$ is observed with a more pronounced number of samples concentrated around the predicted phage coexistence equilibrium value in (e). Panels (f) and (g) correspond to the bacteria and phage community for $K = 10^8$, respectively. The behavior here is identical to that of the previously described simulations.

The results from the numerical simulations displayed in Figure D.1 are consistent with the expected stability from the analysis of prior models. Thus in this system the bacteria only

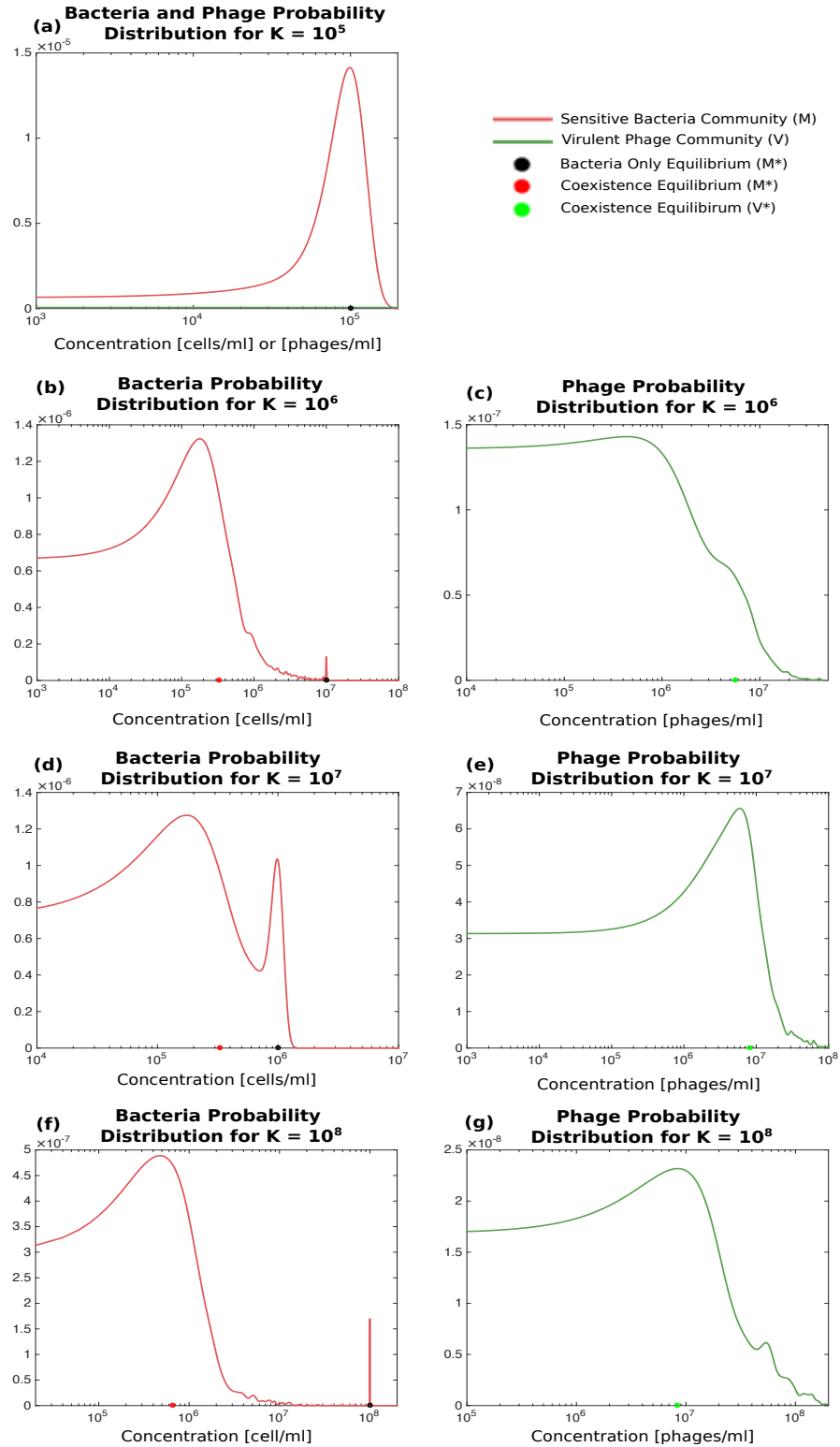


Figure D.1. Kernel probability distributions from simulations of the lytic world community using $n = 2$. MATLAB's ode45 solver was used to determine the final concentrations of the system for 10^3 parameter samples.

equilibrium is stable when $K < \frac{mn}{cd}$ and the coexistence equilibrium is stable when $K > \frac{mn}{cd}$. Even taking into account the chance of numerical error in the simulations, the author is confident that the stability is correct. A more rigorous method of determining the stability in this system could be completed in the future.

D.2 LYSOGENIC COMMUNITY WORLD

A stability analysis of all equilibria in the lysogenic community world is performed. The model in question is given by Equation (4.9) and is reproduced below:

$$\begin{aligned}\frac{dL_i}{dt} &= r \left(1 - \frac{L}{K} \right) L_i - \beta L_i, \\ \frac{dT_i}{dt} &= c\beta L_i - mT_i - \chi dT_i L_i,\end{aligned}\tag{D.6}$$

where $i = 1, 2, \dots, n$.

D.2.1 Equilibria

Setting $\frac{dL_i}{dt} = \frac{dT_i}{dt} = 0$ reveals that there are two combinations of populations of lysogen and phage species for which the system is at equilibrium. The first is the trivial equilibrium, given by $(L_i^*, T_i^*) = (0, 0)$. The second equilibrium represents coexistence in the systems and the population of the lysogen community is given by

$$L^* = \left(1 - \frac{\beta}{r} \right) K.\tag{D.7}$$

In the system the populations of individual lysogen species are not given explicitly, but can be determined from the ratio of $\frac{dL_i}{dt}$ and $\frac{dL}{dt}$. This ratio gives the following differential equation

$$\frac{dL_i}{dL} = \frac{(r(1 - \frac{L}{K}) - \beta)L_i}{(r(1 - \frac{L}{K}) - \beta)L} = \frac{L_i}{L}.$$

Separating variables and letting the initial conditions be $L_i(t_0) = L_{i0}$ and $L(t_0) = L_0$, the solution is given by

$$\frac{L_i(t)}{L(t)} = \frac{L_{i0}}{L_0}.$$

This solution implies that the distribution of lysogen species is invariant in time and is determined by the initial distribution of species.

The population of temperate phage species at the coexistence equilibrium is given by

$$T_i^* = \frac{c\beta L_i^*}{m + \chi dL_i^*}.\tag{D.8}$$

The population of the temperate phage community cannot be determined explicitly because it depends on the distribution of the lysogen species.

D.2.2 Stability

The Jacobian matrix of Equation (D.6) is given by the following:

$$J|_{(L_i, T_i)} = \left(\begin{array}{cccc|cccc} r(1 - \frac{L}{K}) - \frac{rL_1}{K} - \beta & -\frac{rL_1}{K} & \cdots & \cdots & -\frac{rL_1}{K} & & & \\ -\frac{rL_2}{K} & \ddots & & & -\frac{rL_2}{K} & & & \\ \vdots & & r(1 - \frac{L}{K}) - \frac{rL_i}{K} - \beta & & \vdots & & & \\ \vdots & & & \ddots & -\frac{rL_{n-1}}{K} & & & \\ -\frac{rL_n}{K} & & & & r(1 - \frac{L}{K}) - \frac{rL_n}{K} - \beta & & & \\ \hline & c\beta - \chi dT_1 & & & 0 & -m - \chi dL_1 & & 0 \\ & & \ddots & & & & \ddots & \\ & & & c\beta - \chi dT_i & & & & -m - \chi dL_i \\ & & & & \ddots & & & \\ & 0 & & & c\beta - \chi dT_n & & 0 & -m - \chi dL_n \end{array} \right).$$

For the trivial equilibrium, $(L_i^*, T_i^*) = (0, 0)$, the Jacobian matrix evaluates to the following:

$$J|_{(0,0)} = \left(\begin{array}{ccc|ccc} \ddots & & 0 & & & \\ & r - \beta & & & \mathbf{0} & \\ 0 & & \ddots & & & \\ \hline \ddots & & 0 & \ddots & & 0 \\ & c\beta & & & -m & \\ 0 & & \ddots & 0 & & \ddots \end{array} \right),$$

and the eigenvalues are given by $\lambda_i = r - \beta$, for $i = 1, \dots, n$ and $\lambda_i = -m$ for $i = n + 1, \dots, 2n$. Using environmental parameter values for r and β given in Table E.1 reveals that the first n eigenvalues of this matrix are always positive. An application of Theorem A.2 implies that the trivial equilibrium is always unstable.

For the coexistence equilibrium, $(L_i^*, T_i^*) = \left(L_i^*, \frac{c\beta L_i^*}{m + \chi d L_i^*} \right)$, using $L^* = \left(1 - \frac{\beta}{r} \right) K$ the Jacobian matrix evaluates to the following:

$$J|_{(L_i^*, T_i^*)} = \left(\begin{array}{c|c} \begin{array}{cccc} \frac{-rL_1^*}{K} & \dots & \dots & \frac{-rL_1^*}{K} \\ \frac{-rL_2^*}{K} & \ddots & & \frac{-rL_2^*}{K} \\ & & \frac{-rL_i^*}{K} & \vdots \\ \vdots & & & \ddots \\ \frac{-rL_n^*}{K} & & & \frac{-rL_n^*}{K} \end{array} & \begin{array}{c} 0 \\ \\ \\ \\ 0 \end{array} \\ \hline \begin{array}{cc} c\beta - \frac{c\beta L_1^*}{m+\chi dL_1^*} & 0 \\ & \ddots \\ & c\beta - \frac{c\beta L_i^*}{m+\chi dL_i^*} \\ & \ddots \\ 0 & c\beta - \frac{c\beta L_n^*}{m+\chi dL_n^*} \end{array} & \begin{array}{cc} -m - \chi dL_1 & 0 \\ & \ddots \\ & -m - \chi dL_i \\ & \ddots \\ 0 & -m - \chi dL_n \end{array} \end{array} \right),$$

and the eigenvalues are $\lambda = \beta - r$, $n - 1$ copies of $\lambda = 0$, and $\lambda = -m - \chi dL_i^*$ for $i = 1, \dots, n$. This equilibrium is non-hyperbolic and Theorem A.2 cannot be applied to determine its stability. A numerical stability analysis similar to that completed in Appendix D.1.2 is performed.

This community model is an extension of the lysogenic world and thus it is predicted that the coexistence equilibrium will always be stable. MATLAB's ode45 solver is utilized to test this hypothesis. Simulations are run for $K = 10^5, 10^6, 10^7$ and 10^8 . For each value of K , 10^3 parameter samples are created using a Latin Hypercube Sampling Scheme (Appendix E). For each parameter sample Equation (D.6) is solved over a large time span ($t \in [0, 10^3]$ hours). The stability of the equilibrium is identical for all $n > 1$, thus $n = 2$ is chosen to save computation time. The final concentrations of each population are saved from each simulation. A kernel probability distribution is then fit to this data for each value of K . The probability distributions are given in Figure D.2.

To compare the probability distributions to the predicted stable equilibrium points, 10^3 parameter samples are created using the Latin Hypercube Sampling Scheme (Appendix E) and the average value for each parameter is calculated. The values of Equation (D.7) and the equidistributed population for T^* (See Section 4.2)) are found using the average parameter values and plotted with the probability distribution on the x -axis plots as black data points.

It is clear from panels (a), (c), (e), and (g) that the simulations return the expected value for the lysogen population for all K values tested. In panels (b), (d), (f), and (h) the returned values from the simulation are near the expected value for the temperate phage population. This is to be expected as the population of the temperate phage community is approximated by the equidistributed case.

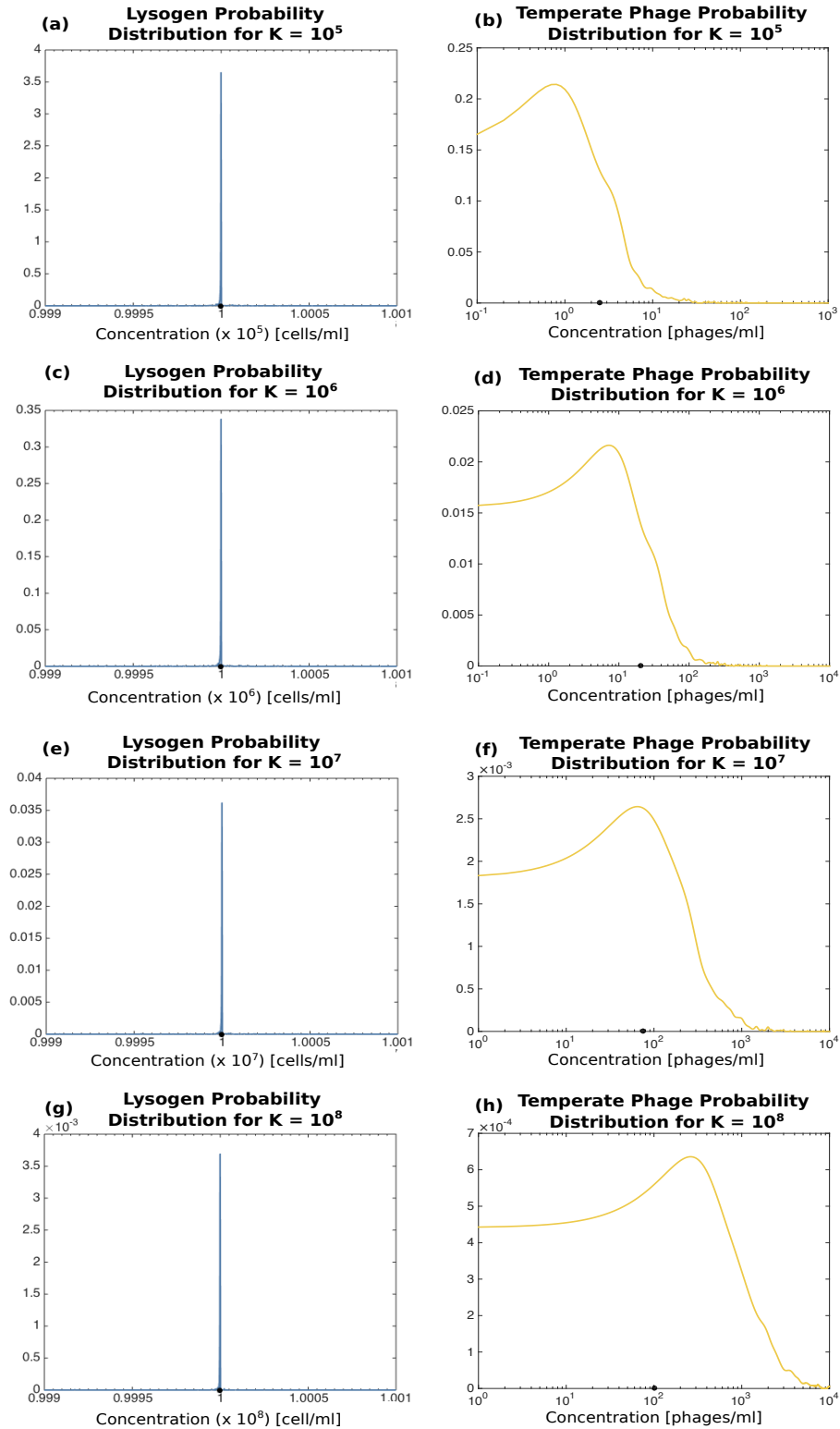


Figure D.2. Kernel probability distributions from simulations of the lysogenic world community using $n = 2$. MATLAB's ode45 solver was used to determine the final concentrations of the system for 10^3 parameter samples.

The results from the numerical simulations displayed in Figure D.2 are consistent with the expected stability from the analysis of prior models. Therefore the coexistence equilibrium is always stable in this system. Even taking into account the chance of numerical error in the simulations, the author is confident that the stability is correct. A more rigorous method of determining the stability in this system could be completed in the future.

APPENDIX E
LATIN HYPERCUBE SAMPLING

LATIN HYPERCUBE SAMPLING

The variability in parameter values is simulated in order to explore the dynamics of the systems studied in this thesis. Parameter measurements across different environments can return different values for the same parameter. It is therefore not satisfactory to choose only one set of parameters to test in the models. To make the results of this analysis more general, a sampling approach is taken. Here a Latin Hypercube Sampling Scheme is used [15, 34, 37]. In this scheme the inputs, $\mathbf{X} = (X_1, X_2, \dots, X_k)$ are treated as random variables with a known probability distribution $F(\mathbf{x})$ for $\mathbf{x} \in S$, where S is the sample space of \mathbf{X} . The output variable is given as $Y = h(\mathbf{X})$ where h is some transformation. The range of each X_i , where $i = 1, 2, \dots, k$, is partitioned into N equal sections. N represents the desired sample size. The probability for each section in the partitioned space is thus given by $1/N$. Sections are sampled from exactly once, and the process of randomly matching samples for each X_i ensures that the entire range for each component is represented.

In the context of this thesis the inputs are the parameters of a model, say $\mathbf{p} = (p_1, p_2, \dots, p_k)$, and the outputs are the equilibrium populations. For each parameter, p_i , where $i = 1, 2, \dots, k$, a baseline value, p_i^* , is chosen. The range for each parameter is then defined by $p_i \in [p_i^* \times 10^{-1}, p_i^* \times 10^1]$. The scheme is implemented in MATLAB and returns N combinations of parameter values which cover the entire sample space of \mathbf{p} . Table E.1 gives the baseline values used in this thesis for parameters that require sampling.

Table E.1. Baseline Parameter Values Used in Latin Hypercube Sampling

Parameter	Value
r	$1/24 \text{ hr}^{-1}$
d	$10^{-8} \text{ ml/cell/hr}$
c	20 virons
m	$1/6 \text{ hr}^{-1}$
β	$1/24 \times 10^{-6} \text{ hr}^{-1}$
s	$1/24 \times 10^{-5} \text{ hr}^{-1}$